INTERNATIONAL ATOMIC ENERGY AGENCY
UNITED NATIONS EDUCATIONAL, SCIENTIFIC AND CULTURAL ORGANIZATION
INTERNATIONAL CENTRE FOR THEORETICAL PHYSICS
I.C.T.P., P.O. BOX 586, 34100 TRIESTE, ITALY, CABLE: CENTRATOM TRIESTE

H4.SMR/942-20

Third Workshop on
3D Modelling of Seismic Waves Generation
Propagation and their Inversion

4 - 15 November 1996

Source Mechanism of Earthquakes from Seismic Waves

A. Udias and E. Buforn

Dept. of Geofisica
Universidad Complutense
Madrid

SOURCE MECHANISM OF EARTHQUAKES FROM SEISMIC WAVES

Agustín Udías and Elisa Buforn

Dpto de Geofísica, Universidad Complutense, Madrid

1. SOURCE MODELS OF EARTHQUAKES

1.1. Kinematic and dynamic models

Once it was accepted that the mechanism of an earthquake is that of a fracture of the material of the earth crust, a quest was started to search for adequate mathematical and physical models or representations of the source, in such a way, that the elastic displacements can be derived from them. These source models or representation are defined by a small number of parameters. One can, then, for a particular earthquake determine these parameters from the observed elastic displacement field, that is, from the observed seismic waves recorded in seismograms. The fracture phenomenon can, in general, be considered from two different points of view: kinematic or dynamic (Aki and Richards, 1980; Udías, 1991). The kinematic models are those that assume the characteristics of the slip or displacement discontinuity at the fault plane. These models are relatively simple and the elastic displacement radiation field can be derived from them. The dynamic models present a much more difficult problem. They try to relate the fracture process to the stress conditions and the material properties at the source region.

1.2 Point source equivalent forces

The first paper that proposed a mathematical representation for the model of the source of an earthquake is that of Nakano (1923) who based his work on that of Love (1920) and Lamb (1904). Nakano tried to find a model that would produce a quadrantal distribution of compressions and dilatations for the first impulses of P waves. His models consist on sets of forces acting at a point of a homogeneous isotropic medium and he calculated the displacement field corresponding to them. Among the models he studied , two, the single couple, and the double couple without moment had a long history. Honda and other japanese authors developed Nakano's ideas (Honda 1962) . He calls these two systems the type I and type II force systems and, following Sezawa and Kanai (1932) expressed the displacement field in spherical coordinates. Point source force models were also developed by Russian seismologists leaded by Keylis-Borok that developed several other source types (Keylis-Borok et al., 1957).

All these formulations have in common that they view the model of the source of an earthquake as a system of forces, mainly couples, acting at a point. From them, the displacements for the seismic waves can be deduced. The equation of motion for the elastic displacements in an infinite, homogeneous, medium for forces **F** acting at a point, using tensor notation, is

$$C_{ijkl}\, u_{k,lj} + F_i = \rho \ddot{u}_i \qquad (1.1)$$

Where C_{ijkl} are the elastic constants and ρ the density of the medium. The indexes after the commas represent derivatives with respect to the space coordinates and repeated indexes are summed. The point force **F** can be considered as the limit of a distribution of forces acting on a volume V, as it is shrunk to a point.

$$F_i(t) = \lim_{V \to 0} \int_V F_i(t,\xi_i)\, dV \qquad (1.2)$$

In the simplest case, equation (1.1) is solved for a single force acting in a particular direction . An expression for the displacements u_i caused by a force in the j direction can be written in the form (Knopoff and Gilbert, 1960)

$$u_i^j = \frac{1}{4\pi\rho}\left[\frac{1}{r\alpha^2}\gamma_i\gamma_j F(t - r/\alpha) - \frac{1}{r\beta^2}(\gamma_j\gamma_i - \delta_{ij})\right.$$

$$\left. F(t - r/\beta) + \frac{1}{r^3}(3\gamma_i\gamma_j - \delta_{ij})\int_{r/\beta}^{r/\alpha} \tau\, F(t - \tau)\, d\tau\right] \qquad (1.3)$$

Where γ_i are the direction cosines of the line from the source to the observation point, r the distance and α and β the velocities of the P and S waves. The index j defines the direction of the force.

The dependence on time of the force must be specified. This can be a harmonic function or, more realistically, some kind of impulsive function, such as a Heaviside step function. The solution can be separated into two parts , the far-field and the near-field. The former correspond to the displacements far away from the source , and contains only the part with the lowest inverse power of the distance, the first two terms of (1.3). This part of the solution is used in the studies of the source from observations at teleseismic distances. Near-field displacements include also the third term of (1.3). The solutions for the infinite, homogeneous medium only give the displacements of the P and S waves.

From the displacements due to a force, those due to a couple of forces can be derived. If u_i^1 are the displacements produced by a force acting along the x_1 axis, those for a single couple in the x_1,x_2 plane with forces along the x_1 axis, are

$$u_i^{SC} = u_{i,2}^1 \qquad (1.4)$$

and for a double couple , with the forces acting along the axes x_1 and x_2 ,

$$u_i^{DC} = u_{i,2}^1 + u_{i,1}^2 \qquad (1.5)$$

Displacements due to other combinations of forces can be deduced in a similar manner.

The two models of point forces that became more widely used to represent the source of an earthquake, were the single and double couple, since both of them give a quadrant distribution of compressions and dilatations for P waves, in agreement with the observations (Fig. 1.1). The double couple system is equivalent to forces of compression and tensional character at 45 degrees of the couples (Fig 1.2). The relation between these models and the physical problem of a fault was at first rather qualitative. Wrongly, the single couple was thought by some authors to

represent the motion of the two sides of a fault. The fault plane would, then, correspond to the plane normal to that containing the forces. In the case of the double couple model, there are two possibilities for the fault plane.

The controversy about which of the two models best represents the source of an earthquake was to be solved comparing the theoretical and observed radiation patterns of seismic waves. Both models give the same radiation pattern for P waves, but not for the S waves (Fig 1.1). As related by Stauder (1962), early studies by Russian seismologists, using the patterns of first motions of SV and SH waves seemed to have proved the adequacy of the single-couple model, although the results of the direction of the S waves presented by Honda agreed with the double-couple model. At that time, the problem seemed to be caused by the poor quality of the seismic data. In the 1960's, after the establishment of the WWSSN stations, good quality, long period S wave data showed abundant evidence in favor of an agreement with the expected radiation pattern of the double-couple source (Khattri, 1973).

The point source force models were also used to calculate the radiation pattern of surface waves that could, in this way, also be used in the retrieval of the source parameters. The first work in this direction seems to be that of Yanovskaya (1958) who calculated the response of a layer over a half-space to Love and Rayleigh waves, for single forces and couples. Ben-Menahem and Harkrider (1964), Harkrider (1964) and Saito (1967) calculated the radiation patterns for surface waves, Love and Rayleigh in a flat stratified earth for buried point sources of single and double couple type. They gave the radiation patterns for amplitudes and phases corresponding to different depths of focus and for different periods.

Generally, the point source force model is used to calculate only the orientation of the source. In the case of the double-couple (DC) model, this is given by the unit vectors in the direction of each couple (X and Y axes). Because of the orthogonality condition only three parameters are necessary to represent the orientation of the source, namely, Φ_x, Θ_x, Φ_y, where Φ and Θ are spherical coordinates measured from north and vertical downward . For the equivalent P and T system , the source parameters are Φ_T, Θ_T, Φ_P .The two normal planes to the plane containing the forces are the two possible fault planes. The orientation of the fault plane is given by the angles ϕ, δ, λ, strike, dip and rake or slip of the motion on each plane (Fig. 1.3). Many methods for the determination of the focal mechanism are based on this simple model and provide these three parameters. The double couple (DC) point source is still a good first approximation to the source of an earthquake when observed at the far field with low frequency waves.

1.3. Kinematic models. Dislocations

The physical model of a fault as the source of an earthquake led to the application of results from dislocation theory to this problem. The earliest ideas on elastic dislocations were proposed by Volterra (1907) and later developed by Nabarro (1951). Applications to the representation of the source of earthquakes were first made by Vvedenskaya (1956, 1959) who considered that the formation of a rupture, or displacement discontinuity in the focus led to an instantaneous removal of stresses over the fault surface. She developed the displacement fields due to several types of faults. The problem was also treated by Steketee (1958), Knopoff and Gilbert (1960) and Maruyama (1963, 1966) who also showed the equivalence between dislocations and body forces. This problem was solved in a more general form by Burridge and Knopoff (1964). They used a representation theorem in terms of the Green's function that had been introduced by the previous work of de Hoop (1958) and has, since, become the standard way to present the equations of the displacement field in source mechanism studies. The Green's function in elastodynamics represents the displacements corresponding to a unit force in an arbitrary orientation impulsive in space and time. For an infinite, homogeneous medium, the Green's function G_{ij} is given by equation (1.3), substituting $F(t)$ for $\delta(t)$, the Dirac's delta function.

A dislocation is an internal surface across which there is some kind of discontinuity in displacement or stress. Let us consider the case in which the medium is infinite, there are no body forces, and across and internal surface Σ there is continuity of stress and a discontinuity of displacements, given by $\Delta u_i(\xi_i,t)$, which is usually called the slip of the fault (Fig. 1.4). Using the representation theorem in terms of the Green's function, the displacements $u_i(x_j,t)$ for any point of the medium can be written in the form

$$u_n(x_s,t) = \int_{-\infty}^{\infty} d\tau \int_{\Sigma} \Delta u_i(\xi_s,\tau) C_{ijkl} G_{nk,l}(x_s,t,\xi_s,\tau)\, n_j(\xi_s)\, dS \qquad (1.6)$$

Where n_j is the unit vector normal at each point of the surface Σ, C_{ijkl} the elastic constants of the medium and $G_{nk,l}$ the derivatives of the Green's function. For a shear dislocation in an isotropic medium, if the slip is in a constant direction given by the unit vector l_i, equation (1.6) becomes

$$u_k = \int_{-\infty}^{\infty} d\tau \int_{\Sigma} \mu\, \Delta u\, (l_i n_j + l_j n_i)\, G_{ki,j}\, dS \qquad (1.7)$$

This expression gives the elastic displacements at any point of the medium, in terms of the slip on the fault plane Σ and the Green's function. The orientation of the source is given by that of the unit vectors l_i and n_i. Since in (1.7) we can interchange these two vectors with the same result for u_k, this means that there are two perpendicular faults that result in the same displacement field. This ambiguity is inherent to the problem itself. A shear dislocation has been shown to be equivalent to a distribution of double-couple point forces on the fault plane (Burridge and Knopoff, 1964). In equation (1.7), the time dependence of slip must be specified, often a step Heaviside function is used. If the displacements u_i are observed at large distance compared with the fault dimensions and for large wave lengths, the source may be considered as a point, and the displacements are given by the time convolution of the slip function with the derivatives of the Green function. For the point source approximation a pure shear dislocation is equivalent to a double-couple (Fig. 1.2).

For a point shear dislocation with slip Δu depending on time, the far field for the P and S waves in an infinite homogeneous medium is given by

$$u_k^P = \frac{\mu S}{4\pi\rho\alpha^2 r} \gamma_j \gamma_k \gamma_l (n_l l_j + n_j l_l) \Delta\dot{u}(t - \frac{r}{\alpha}) \qquad (1.8)$$

$$u_k^S = \frac{\mu S}{4\pi\rho\beta^2 r} (\gamma_i \gamma_k - \delta_{ik}) \gamma_j (n_l l_j + n_j l_l) \Delta\dot{u}(t - \frac{r}{\beta}) \qquad (1.9)$$

Where S is the area of the dislocation, μ the shear modulus, and γ_i the direction cosines of the line from the source to the observation point at a distance r. It is important to notice that the displacements u depend on the slip velocity $\Delta\dot{u}$ and not on the slip itself. The source ceases to radiate energy when $\Delta\dot{u} = 0$.

The representation theorem can also be applied to distributions of body forces over a volume V in the form,

$$u_n(x_s,t) = \int_{-\infty}^{\infty} d\tau \int_V F_i(\xi_s,\tau)\, G_{ni}(x_s,t;\, \xi_s,\tau)\, dV \qquad (1.10)$$

In this form, the equivalent body forces can be found for different kinds of dislocations. In equations (1.6) and (1.10) homogeneous initial and external boundary conditions are assumed. This representation of the displacement field is very useful, since it allows a rapid calculation of the displacements for a variety of source types and orientations once the Green's function has been determined for a particular medium.

1.4. Determination of source mechanism parameters

Seismological methods for the determination of the parameters that define the mechanism of earthquakes are based on the analysis of observations of seismic waves. In general, this leads to an inverse problem: given a set of observations, the values of a set of source parameters are sought which best fit the observations. The parameters depend on the model used to represent the mechanism of the source. In this way, the methods to determine the source parameters are based on the development of the theory of the source representation. The direct problem, that is, the equations that gives the elastic displacements field corresponding to a given source model, must be first solved. Since the seismic waves must propagate from the source to the point of observation through the earth, its structure must be known in advance. The fact that our knowledge of the properties of the propagating medium is always imperfect, imposes certain limits to our knowledge of the source. Which characteristics of the seismic signal under study are due to the source and which are due to the medium is a problem always present. In general, there is a trade-off between the details of the source that are sought and the details of the structure of the medium that must be assumed to be known. Simple models of the source, observed at long distance and low frequencies, are little affected by the propagating effects. On the contrary, the complex models observed at near distances and at high frequencies are more affected by the structure of the earth crust.

1.5 Signs of first motions of P-waves

The first methods to study the source mechanism of earthquakes were based on the observations of the compressional or dilatational nature of the first impulse of the P-waves. Because of the simplicity of this type of data, these methods are still

widely used. One of the first indications that there may be a connection between this type of observations and the mechanism of earthquakes was made by Walker in 1912. The first to identified the quadrant distribution of compressions and dilatations was Shida in 1917 (Kawasumi, 1937). The first working method was developed by Byerly in 1928. He accepted Reid's elastic rebound theory and used the theoretical results of Nakano (1923), assuming a single couple of forces as the source model. To reduce the observations to a homogeneous medium, he introduced the concept of extended positions. The method consists in the separation of the regions of compressions and dilatations by two orthogonal nodal planes, the fault plane and the auxiliary plane. The problem was solved in a graphical way, plotting the observations at their extended positions on a stereographic projection, with the anticenter as the pole. On this projection, the nodal planes project as circles. From this representation, the strikes and dips of the two nodal planes can be determined. From the method itself, one cannot identify the fault plane from the auxiliary plane. Byerly's method, known as the fault-plane solution, was rapidly adopted as a standard method for the study of the mechanism of earthquakes.

Independently of Byerly's work, studies of the mechanism of earthquakes using first-motion data were also pursued in Japan and Europe. An important contribution from these two groups is the use of the focal sphere. The focal sphere is used to project the observations to points on the surface of a sphere of unit radius and homogeneous material around the focus simplifying the solution of the problem. Ritsema (1955), based on early work by Koning (1942), was the first to carry out the complete determination of the fault-plane solution using the Wulff-net projection of the focal sphere. In Japan, the focal sphere was initially used to represent the results of the analysis performed on geographical maps, and later to plot the data and solve the problem using a Schmidt equal-area stereographic projection (Honda, 1962) . In the Soviet Union , since the middle 1950, seismologists use a Wulff-net projection of the focal sphere to plot first motion polarities of P, SV and SH waves and their corresponding nodal lines (Keylis-Borok, 1956). Another projection used by Stauder is the central projection, where the nodal planes project as straight lines (Stauder, 1962). The equivalence of the different representations and projections was shown by Scheidegger (1957).

1.6 Geometry of the source

The orientation of the slip on a fault plane is given by the unit vectors **n** (normal to the fault) and **l** (direction of slip) or by the angles ϕ, δ y λ (fig. 1.3)

ϕ = Azimuth of the trace of the fault plane, measured from 0° to 360° clockwise from North, so that the dip falls to the right

hand.

δ = Dip of the fault plane from 0° to 90°, measured from the horizontal

λ = slip angle from -180° to 180° from the horizontal to the direction of the slip on the fault plane, in such a way that the dip falls on the right hand of the azimuth.

The relation between the system of axes of the forces (double couple) X, Y, Z, with the principal axes of stresses P, T, Z are (Buforn, 1985).

$$\begin{pmatrix} \alpha_x \\ \beta_x \\ \gamma_x \end{pmatrix} = B^T \begin{pmatrix} 1/\sqrt{2} \\ 1/\sqrt{2} \\ 0 \end{pmatrix} \qquad (1.11)$$

$$\begin{pmatrix} \alpha_y \\ \beta_y \\ \gamma_y \end{pmatrix} = B^T \begin{pmatrix} 1/\sqrt{2} \\ -1/\sqrt{2} \\ 0 \end{pmatrix} \qquad (1.12)$$

Where B is the matrix of the direction cosines of the axes T, P, Z.

$$B = \begin{Bmatrix} \alpha_T & \beta_T & \gamma_T \\ \alpha_P & \beta_P & \gamma_P \\ \alpha_Z & \beta_Z & \gamma_Z \end{Bmatrix} \qquad (1.13)$$

Due to the orthogonality of the axes only three angles are needed to define the orientation of each axis:for example, Θ_T, Φ_T y Φ_P, or of a plane ϕ, δ y λ. The relation between these parameters are

$$\phi = \Phi_x + \pi/2$$

$$\delta = \Theta_x \qquad (1.14)$$

$$\lambda = \text{sen}^{-1}\left(\frac{\cos \Theta_y}{\text{sen } \Theta_x} \right)$$

To correct for the heterogeneities of the earth, observations are projected on to the surface of the focal sphere. Each point of observation (station) projected tracing back along the seismic ray to the focus, where its position is given by the polar angles i_h y Φ (Fig. 1.5).

i_h = Incidence angle at the focus, measured from the vertical downward from 0 to 180°.

Φ = Azimuth from epicenter to station measured clockwise from North from 0 to 360°.

Determination of the incidence angle in the focus (take-off angle) depends on the earth structure. For large (teleseismic) distances (Δ > 1000 km), i_h can be determined from the travel-time curve. For a focus at depth h the relation is

$$\text{seni}_h = \frac{v_h \; dt}{r_h \; d\Delta} \qquad (1.15)$$

Determination is usually done by computer programs that determine i_h from the Jeffreys-Bullen tables. In the case of short distances (Δ < 1000 km), determination of i_h implies the knowledge of crustal and upper mantle models for the particular region. One type of model recommended is one formed by linear gradients of velocity. For these models i_h varies in continuous form with distance. In the models of layers with constant velocity i_h has discontinuities.

Once the observations are projected on the surface of the focal sphere, the method consists in separating them into four quadrants of alternating compressions and dilatations with two orthogonal planes. The solution of the problem may be done in graphic or numerical form. Graphic solutions may be done using a stereographic net or representing it on the screen of a computer.

1.7 Graphic methods

The data for the graphic solution of the problem are for each station P wave polarities, dilatations or compressions, azimuth from the epicenter to the station and incidence angle in the focus or take-off angle . The solution is made on a stereographic projection of the focal sphere (Schmidt or Wulff net). Generally, the lower hemisphere of the focal sphere is projected ($0^\circ \leq i_h \leq 90^\circ$) for this reason the upgoing rays ($i_h' > 90^\circ$) must be projected on the lower hemisphere

$$i_h = \pi - i_h'$$
$$\Phi = \Phi' + \pi \qquad (1.16)$$

Each station is located on the focal sphere in the following manner: the azimuth Φ is measured from North clockwise, and the take-off angle i_h from the vertical downward, that is from the center of the projection. At each station, a different symbol is used, a black circle for compressions and a white one or a triangle for dilatations. In Figure 1.6, the following stations are represented.

Station	Φ	i_h	P
ST1	40	60	D
ST2	120	30	C
ST3	212	50	D
ST4	310	80	C

Once all observations are situated on the projection of the focal sphere, compressions and dilatations are separated by one of the great circles of the net, this is called the plane A. This circle is drawn and its pole, that is the X axis is located. The

pole is located at 90° normal to the plane A (Fig. 1.6) The second plane, plane B, must pass through the pole of the plane A, X axis and separate the compressions and dilatations in four alternating quadrants. The pole of the plane B must fall on the plane A, so that the two planes are orthogonal. The Z axis (null axis) is located at the intersection of the two planes. The axes of Pressure and Tension (P and T) are located at a great circle that passes through the axes X and Y and at 45° from them. The T axis is located at the compressions quadrant and the P axis at the dilatations quadrant (Fig. 1.6). Once the planes A and B, and the axes X, Y, Z, P and T are located the angles ϕ azimuth, δ dip and λ slip, for each of the two planes and for each of the five axes the angles Φ and θ are measured. The values corresponding to the solution of Figure 1.6 are:

	Φ	θ
P	20	82
T	120	40

The orientation of planes A and B is given by the angles ϕ, δ, λ which are obtained from the projection in the following form:

ϕ : Azimuth is measured from 0 to 360, from North clockwise to the intersection of the plane with the horizontal (limit of the net) which has the dip of the plane to the right.

δ : dip measured from 0 to 90 from the horizontal (from the limit of the net toward the center) at 90° from ϕ.

λ : Slip mesured from -180 to 180 from the horizontal starting at the azimuth ϕ along the plane to the pole of the other plane (in plane A to Y axis and in plane B to X axis). The angle is positive if the center of the projection falls on the compressional quadrant (reverse fault) negative if it falls on the dilatational quadrant (normal fault).

For the solution of Figure 1.6, these values are:

	ϕ	δ	λ
plane A	146	50	35
plane B	260	64	134

The graphic determination can be also made in an interactive manner on the screen of a computer. Data needed are the same as in the case of the manual solution. For this purpose Buforn (1994)

has written a useful program. Station data (ϕ, i_h, +1 or -1) (+1 compressions, -1 dilations) are entered in the computer or read in a file. The program situates them on the projection of the focal sphere and show them on the screen. A series of options allows to give as a possible solution the axes P and T, X and Y or the planes A and B. The program adjust the orthogonality of axes and planes. The program draws the planes on the screen and calculate the score of the solution (proportion of correct data). Examining the solution on the screen and the value of the score, new values for for the orientation of axes or planes are given until the solution is found satisfactory (maximum value of the score).

1.8 Numerical methods

With the advent of computers, the question soon arose of applying numerical methods to the fault-plane problem. The first workable formulation of the problem was presented by Knopoff (1961). The solution is given by the orientation of the source which correspond to a maximum probability of correct readings. The function to be maximized is

$$\Phi = \sum_{i=1}^{N} \log \frac{1}{2} [\, 1 + \mathrm{erf}(U_i/\alpha)\ \mathrm{sgn}\ U_i\ \mathrm{sgn}\ R_i \,] \qquad (1.17)$$

Where U_i are the theoretical and R_i the observed amplitudes of P waves and α, a constant that represents the noise level. The problem was solved using a projection of the observations into an antipodal plane of the epicenter. The problem was reformulated by Kasahara (1963) using spherical coordinates in the focal sphere, weights for the stations and a method of successive approximations from an initial solution. The basic ideas of Knopoff and Kasahara were used in a computer program developed by Wickens and Hodgson (1967) in a modified way. This program was used extensively in the Dominion Observatory (Canada) in a reevaluation of the fault-plane solutions for the period 1922 to 1962.

A probabilistic formulation of the problem was proposed by Keilis-Borok et al. (1972) using a maximum likelihood method. If π_k is the probability of a correct reading with respect to the expected sign α_k from a given source orientation, the likehood function is given by

$$L = \sum_{k=1} \pi_k^{(\alpha_k + 1)/2} (1 - \pi_k)^{(\alpha_k - 1)/2} \qquad (1.18)$$

α_k is a function of the three angles that define the orientation of the source. Maximum likelihood estimates of these parameters are found by the maximization of L.

A very useful numerical method was developed by Brillinger, Udías and Bolt (1980) and Udías and Buforn (1988). In this method the probability of reading a compression is given as a function of the expected amplitude of the P waves $A(\phi,\delta,\lambda)$

$$\pi_i = \mathrm{prob}(Y_i = 1) = \gamma + (1-2\gamma)\Phi[A_i(\phi,\delta,\lambda)] \qquad (1.19)$$

Where γ has values between 0 and 1/2 and represents reading errors and $\Phi(A)$ is the cumulative error function. The likelihood function is similar to expression (1.18) substituting α_k by Y_k which are now the observed values of the polarities of P waves and π_k by the expression (1.19). The method gives the standard errors of the parameters of the solution. An example of a numerical solution found using this method is given in figure 1.7. This method has been extended by Buforn and Udías (1984) to use also the signs of SH and SV wave first motions.

An extension of the problem to consider fault plane solutions for groups of earthquakes in the same area was also presented by Brillinger et al. (1980). In this case the probability of a correct reading is a function of the expected amplitudes of the P waves and the likelihood function is written in the form

$$L = \sum_{i=1}^{M} \sum_{k=1}^{N_i} \log \frac{1}{2} [\, 1 - (2\,\pi_{ik} - 1)\, Y_{ik} \,] \qquad (1.20)$$

Where M is the number of earthquakes and N_i the number of observations in each earthquake, π_{ik} the probability of reading a compression at station k from shock i , and Y_{ik} the observations

of P wave polarities at station k from shock i. For group solutions the method permits the separation of the shocks into groups, each with the same regional mechanism.

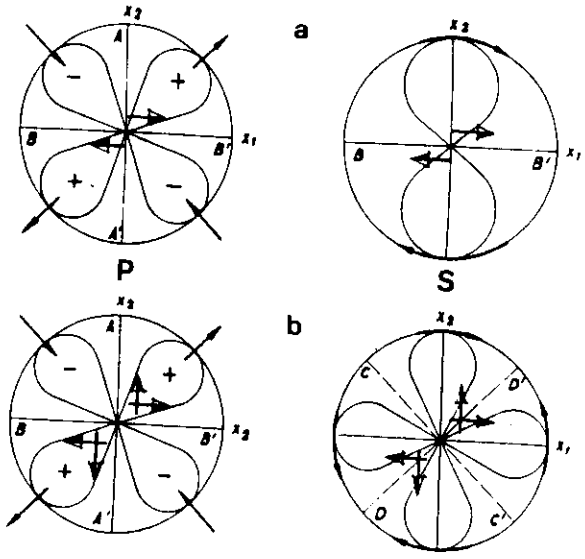

FIG. 1.1

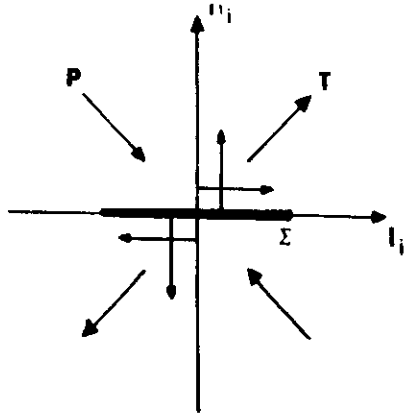

FIG. 1.2

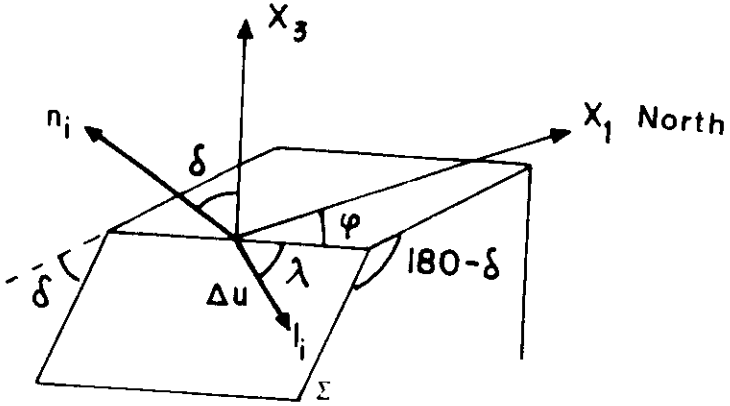

FIG. 1.3

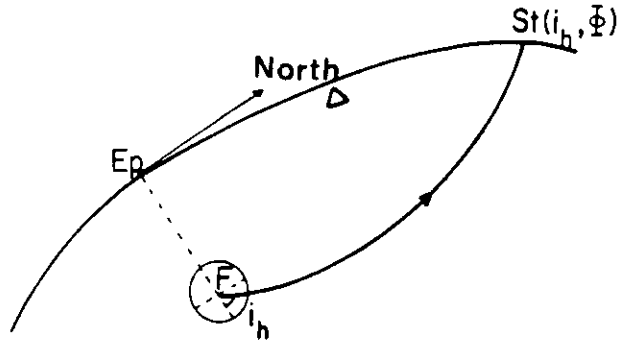

FIG. 1.5

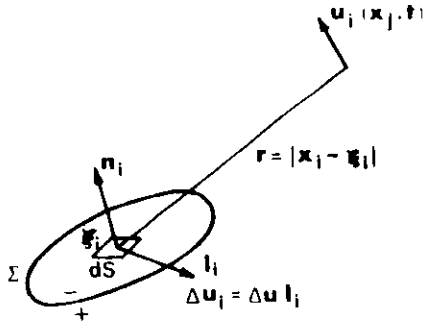

FIG. 1.4

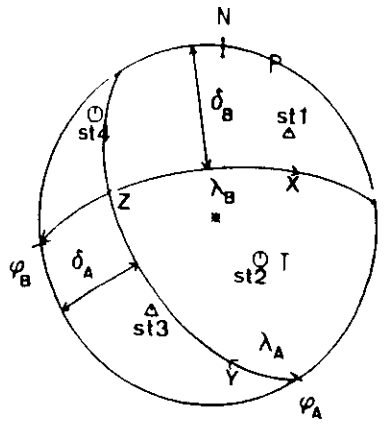

	Θ	Φ
T:	40.00	120.00
P:	81.71	20.00

	φ	δ	λ
A:	145.79	49.94	35.07
B:	260.11	63.91	134.22

FIG. 1.6

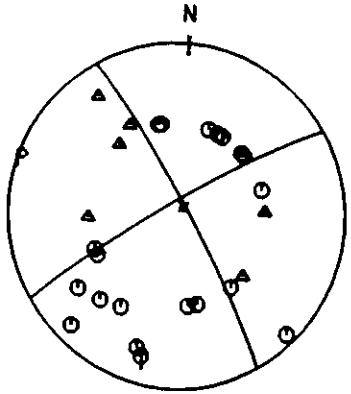

	θ	ϕ
T:	82±7	194±6
P:	85±8	284±6

	φ	δ	λ
A:	239±6	88±13	170±6
B:	329±6	80±6	6±13

N= 29 SCORE= 0.83

FIG. 1.7

2. SEISMIC MOMENT TENSOR

A very important concept in the formulation of the theory of the earthquake source is the seismic moment tensor. The seismic moment tensor was first proposed by Gilbert (1970) defining it as the integral over the focal volume of the stress drop, in such a way, that the body forces can be derived from it. The meaning of the moment tensor was clarified by Backus and Mulcahy (1976) who pointed out to certain confusions in the original formulation. They related the moment tensor to the stress glut or difference between the elastic stresses and the true physical stresses. In other words, it represents the inelastic strain in the source; that is, the internal stress necessary to cancel the strain produced by internal non linear processes (Madariaga, 1983). Geller (1976) showed the relation of the moment tensor to body forces and the expressions of the elastic displacement field in terms of the Green's function, according to the formulation of Burridge and Knopoff (1964).

2.1 Definition

The moment tensor M_{ij} can be expressed as the integral of the moment tensor density m_{ij} over the source volume, or the source surface. The equivalent body forces per unit volume can be shown to be related to the moment tensor in the form

$$f_i = - m_{ij,j} \qquad (2.1)$$

In this way, the moment tensor can represent very general types of force models. The components of M_{ij} corresponds to couples of forces which for i = j, they have the arm in the same direction as the forces and for i ≠ j, perpendicular to them (Fig.2.1). A combination of the resultant 9 couples may represent any type of point source.

For homogeneous initial and boundary conditions, the elastic displacement field for a volume source, in terms of the Green's function, can be written in the form

$$u_k = \int_{-\infty}^{\infty} d\tau \int_V m_{ij} G_{ki,j} \, dV \qquad (2.2)$$

For a surface, the expression is

$$u_k = \int_{-\infty}^{\infty} d\tau \int_{\Sigma} m_{ij} G_{ki,j} \, dS \qquad (2.3)$$

In equation (2.2), m_{ij} represents the moment tensor density per unit volume, while in (2.3) represents the density per unit surface. For a displacement dislocation such as in (1.6) in an isotropic medium, allowing for changes in volume, the moment tensor density is given by

$$m_{ij} = \lambda \Delta u \, n_k l_k \delta_{ij} + \mu \Delta u \, (n_i l_j + n_j l_i) \qquad (2.4)$$

Where n_i and l_j are the unit vectors in the direction normal to the fault surface Σ and in the direction of the slip Δu. The part of (2.4), corresponding to $i = j$, represents changes in volume. If n_i and l_i are perpendicular, the expression represents a pure shear dislocation and is given by

$$m_{ij} = \mu \Delta u \, (n_i l_j + n_j l_i) \qquad (2.5)$$

In this expression, $m_{11} + m_{22} + m_{33} = 0$, which is the condition for a moment tensor without changes in volume.

For the far field, at large distances from the source and for low frequencies, the point source approximation is valid and the displacements may be written in the form

$$u_k = M_{ij} * G_{ik,j} \qquad (2.6)$$

where the star represents the time convolution and M_{ij} is the integral of m_{ij} over the source volume. The resulting expressions for the far field of the P and S waves are

$$u_k^P = \frac{1}{4\pi\rho\alpha^3 r} \gamma_k \gamma_j \gamma_i \dot{M} \left(t_\alpha - \frac{r}{\alpha}\right) \qquad (2.7)$$

$$u_k^S = \frac{-1}{4\pi\rho\beta^3 r} (\gamma_i \gamma_k - \delta_{ik}) \gamma_j \dot{M} \left(t_\beta - \frac{r}{\beta}\right) \qquad (2.8)$$

For a pure shear dislocation, equivalent to a double-couple (DC), $M_{ij}(t)$ is given by

$$M_{ij}(t) = M_0 (n_i l_j + n_j l_i) f(t) \qquad (2.9)$$

M_0 is the scalar seismic moment and f(t) the source time function. Since the displacement field (2.7) and (2.8) depends on the time derivative of the moment tensor, the term source time function is applied to the derivative of f(t).

The scalar moment tensor was first introduced by Aki (1966) for a shear dislocation in the form

$$M_0 = \mu \, \bar{\Delta u} \, S \qquad (2.10)$$

where $\bar{\Delta u}$ is the average value of the slip over the fault surface, μ the rigidity of the source medium and S its area. He also made the first determination of the seismic moment for the Niigata earthquake of 1964, using long period surface waves and found it consistent with field observations of ground rupture.

Since moments are conserved, M_{ij} is symmetric and in general has 6 independent elements. Its eigenvalues σ_1, σ_2, σ_3, are real and, in the general case, have different values. The three eigenvectors are orthogonal and represent the axes of maximum, intermediate, and least moment (P,B,T). For a source with no net change of volume, the moment tensor is purely deviatoric and its trace is zero

$$\sigma_1 + \sigma_2 + \sigma_3 = 0 \qquad (2.11)$$

For a pure shear fault or a DC source, the eigenvalues are

$$\sigma_1 = M_0, \quad \sigma_2 = 0, \quad \sigma_3 = - M_0 \qquad (2.12)$$

This condition implies that the determinant of M_{ij} is zero.

2.2 Partition of moment tensor

In the general case, M_{ij} is a general symmetric tensor and can be separated into an isotropic (change in volume) and a deviatoric part.

$$\mathbf{M} = \mathbf{M}^{ISO} + \mathbf{M}^{DEV} \qquad (2.13)$$

There is good evidence that earthquakes sources are deviatoric with no net-changes in volume. However, a deviatoric moment tensor, in general, does not correspond to a pure DC (double couple or shear fracture) source. For this reason, the deviatoric tensor can be divided into a DC part and another part that is not DC (NDC). Thus a general moment tensor is divided into three parts

$$\mathbf{M} = \mathbf{M}^{ISO} + \mathbf{M}^{DC} + \mathbf{M}^{NDC} \qquad (2.14)$$

The non-DC part may assume several forms. A non-DC deviatoric source was proposed by Randall and Knopoff (1970) which was called the compensated linear vector dipole (CLVD). Physically , this model represents a sudden change in the rigidity at the source. The moment eigenvalues are

$$\sigma_1 = - M_0/2 , \quad \sigma_2 = -M_0/2 , \quad \sigma_3 = M_0 \qquad (2.15)$$

A general deviatoric moment tensor can be separated into a DC component and a non-DC part. This separation can be done in many ways. In the inversion of moment tensors from observations of seismic waves, the source is not restricted to be a DC. The moment tensors obtained are deviatoric tensors and from them the DC part is separated. This separation can be done in terms of a major and a minor double-couple or in what has been called the best double-couple. Strelitz (1989) has shown that most separations can be reduced to the sum of DC + CLVD source components.

$$\mathbf{M} = \mathbf{M}^{ISO} + \mathbf{M}^{DC} + \mathbf{M}^{CLVD} \qquad (2.16)$$

The presence of non-DC components in the moment tensor obtained from seismic observations may also be attributed to heterogeneity and/or anisotropy in the source region. However, this may be also due to errors in the observations or in the earth models used in the inversion and not necessarily to source effects (Sipkin, 1986).

The first order moment tensors are related to point sources. If the characteristics of extended sources are to be described in terms of moment tensor distributions, higher order moments must be used. The first order will define the center of gravity of the source, the second the characteristic size of the source, etc. In practice determining higher order moments is a complicated process. A point source at a known location and origin time is defined by a first order moment tensor and specified by six parameters. If the location and origin time are not known, the source is defined by 10 parameters. An extended source can be represented by second order moment tensor including the time and space derivatives, with 20 parameters related to the location, orientation, rise time, spatial extent and rupture velocity (Doornbos, 1982).

2.3. Moment tensor inversion

Since the earliest formulation of the seismic moment tensor by Gilbert (1970) , it became apparent that the displacements of the seismic waves are a linear combination of the elements of the moment tensor and those of the derivatives of the Green function (2.6). This linearity was first used by Gilbert (1973) for calculating tensor elements from seismic wave observations. This problem is known as moment tensor inversion. The problem of moment tensor inversion can be considered in various parts. First the inversion of first order moment tensor, time independent and time dependent and secondly to the problem of higher order moment tensors. The most common problem refers to the inversion of first order time independent moment tensors. This problem is important because they describe, in a first order approximation, the equivalent forces of a general point source. As it was explained in part 2.1, they correspond to a very general type of source of which the shear dislocation is a particular case. If no restrictions are imposed the inversion of the moment tensor will provide knowledge not only of the orientation of the source, but also of the type of source.

The problem of moment tensor inversion can be treated in the time or frequency domain. The far field displacement for a point source can be expressed in the time domain as a convolution of the derivatives of the Green function with the seismic moment tensor

$$u_i(t) = \int_{-\infty}^{\infty} G_{ij,k}(t - \tau)\, M_{jk}(\tau)\, d\tau \qquad (2.17)$$

and in the frequency domain as the product of their Fourier transforms

$$U_i(\omega) = G_{ij,k}(\omega)\, M_{jk}(\omega) \qquad (2.18)$$

It is , then, possible in both cases to obtain by linear inversion the components of M_{ij}. Since the moment tensor is a symmetric tensor only six of its nine elements are different. If no restrictions are imposed , the source is of general type and may have a component of volume change. This is the isotropic component. If this component is zero, imposing the condition

$$M_{11} + M_{22} + M_{33} = 0 \qquad (2.19)$$

With this condition, the tensor is purely deviatoric and the independent elements are only five. This is a linear condition, and therefore does not affect the linearity of the problem. If the condition that the source corresponds to a shear dislocation (double-couple) is imposed, that is, that the determinant is zero, the problem is no longer linear.

In general, the derivative of the Green's function $G_{ki,j}$ have 27 different components. However, for a purely deviatoric source, only 8 selected combinations are needed. For example, the SH displacements, observed at an azimuth ϕ from the source can be expressed in the form

$$U_k^{SH} = -1/2(G_{k1,2} + G_{k2,1})\sin 2\phi\, (M_{11} + M_{22}) + (G_{k1,2} + G_{k2,1})\cos 2\phi\, M_{12} - (G_{k2,3} + G_{k3,1})\sin\phi\, M_{13} + (G_{k2,3} + G_{k3,1})\cos\phi\, M_{23} \qquad (2.20)$$

If the orientation of the mechanism does not vary with time, then we can separate the source time function f(t)

$$M_{ij}(t) = M_{ij}\, f(t) = M_0\, m_{ij}\, f(t) \qquad (2.21)$$

In equations (2.17) and (2.18) from a set of observations u_k we can determine the mechanism defined by M_{ij} if we know the derivatives of the Green function $G_{ki,j}$ also called the excitation functions of the medium whose elements depend on the Earth model used. For this purpose we have to solve in these two equations for M_{ij}. We write them in matrix form

$$U = G\, M \qquad (2.22)$$

where U(N) is a vector of dimension N (number of observations) M(6) has dimension 6 (the 6 different components of the moment tensor) and G(N × 6) is a matrix of dimension Nx6. In the frequency domain (2.18), the equation can be written for each frequency. The relation is linear for the real and the imaginary parts of U_i . For the modulus , the relation is non-linear and it must be solved through a proper linearization. If the real and imaginary parts of the spectrum are used , for N stations and M frequencies there are 2NM equations to be solved for the 6 components of the moment tensor. The excitation functions must also be known at each station and for each frequency, that is , in general 6NM. Since data from many stations and frequencies are generally used, the problem is overdetermined. The 6 components of M reduce to 5 if we introduce the condition of that there are no changes of volume.

$$M_{11} + M_{22} + M_{33} = 0 \qquad (2.23)$$

Since according to (2.17) and 2.18) we have N equations with 6 unknown, the system is over determined and may be solved by least squares. The solution may be written in the form

$$\mathbf{M}=(\mathbf{G}^T\mathbf{G})^{-1}\mathbf{G}^T\mathbf{U}(2.24)\ \mathbf{M}=(\mathbf{G}^T\mathbf{G})^{-1}\mathbf{G}^T\mathbf{U} \qquad (2.24)$$

Also using Lanczos generalized inverse matrix

$$\mathbf{M} = \mathbf{B}\,\Lambda^{-1}\,\mathbf{V}^T\,\mathbf{U} \qquad (2.25)$$

Where Λ is a diagonal matrix formed by the eigenvalues of **G**, **B** the matrix formed by the eigenvectors of **G** and **V** the matrix formed by the eigenvectors of $\mathbf{G}^T$.

This form of solving the inverse problem has sometimes many difficulties due to the ill conditioned nature of the matrix **G**. For this reason, the problem is often solved in the direct form, given values of **M** and calculating **U**. The error is defined as the difference between the observed and calculated values of **U**. The solution is found as the value of **M** that gives a minimum error in the least square sense. Because of the influence of the depth of the focus h, this parameter is also introduced in the problem as an unknown together with the 5 components of **M**.

Data used are the displacements of internal, surface waves or free oscillations.The inversion can be done in the time (2.21) or frequency domain (2.22). In all cases, we must have in mind that both equations represent the ground displacements, so that the seismograms must be corrected previously for the instrument response. Regarding the Green functions, they must be calculated for a given theoretical Earth model. The simplest one is that of an infinite, homogeneous, isotropic medium. They become more complicated as we complicate the model. The functions depend on the relative position of the observation point with respect to the focus (hypocenter). For teleseismic distances standard Earth models may be used. For regional distances local models of the crust and upper mantle must be used.

In figure 2.2, the focal mechanism obtained from the inversion of the moment tensor using internal waves together with the best DC component. The components of the moment tensor are the

following,

$$m_{11} = 8.90$$

$$m_{12} = 5.80$$

$$m_{13} = 1.10$$

$$m_{22} = -6.60$$

$$m_{23} = 9.93$$

$$m_{33} = -2.30$$

The percentage of non-DC component in the solution is 14.38 %. This is a large amount and it means that the source cannot be considered as a pure shear fracture. This characteristic of the source is lost in other methods where the DC character of the source is assumed from the starting point.

The first procedure for moment tensor inversion was proposed for free oscillations data by Gilbert and Dziewonski (1975). Mendiguren (1977) presented the inversion of surface waves. He used a linear inversion of the real and imaginary parts of the spectra of Rayleigh and Love waves and a linearized procedure for the non-linear problem of the amplitude spectra. The method provides also a fast way to determine the source depth. Some problems involved in the linear inversion were pointed out by Patton and Aki (1981). Kanamori and Given (1981) presented a method using the spectra of long period (180 to 350 s) Rayleigh and Love waves. They pointed out that for shallow sources, the determination of certain components of the moment tensor (M_{13} and M_{23}) becomes very difficult. To overcome this difficulty, they introduced certain constraints. One of them is to force these two components to be equal to zero. This is equivalent to force the mechanism to be a pure strike-slip on a vertical fault or a pure dip-slip on a fault dipping 45 degrees. This may provide a very useful first approximation. Since the solution was not forced to be a double-couple source, it is separated into a major and a minor double-couples.

Romanowicz (1982) proposed a two steps method for moment tensor inversion in the frequency domain. The first step, independent of depth and azimuth solves for 5M unknowns from the total of 2MN equations. The second step uses 5M equations to solve for the 5 unknowns (5 components of deviatoric moment tensor) for different values of the depth. The minimum error selects the value of depth and the corresponding value of the moment tensor.

Stump and Johnson (1977) presented the first inversion of body waves in the time domain. They applied the method to synthetic data and made use of the Lanczos' generalized inverse matrix. Body waves were also used in the inversion of the moment tensor by Strelitz (1978). Amplitudes of teleseismic body waves were used by Fitch et al. (1980) to estimate the elements of the seismic moment tensor. Sipkin (1982) used a method based on multichannel signal enhancement in the time domain. Using recursion techniques, the elements of the moment tensor are solved for, as the optimum multichannel signal-enhancement filter. In a second approach a multichannel vector deconvolution is used in which a set of filters is computed which, when convolved with the data yield time averages of the elements of the moment rate tensor. These methods can be applied to a variety of data of teleseismic and local earthquakes. Sipkin's method is applied in a routine form to sufficiently large earthquakes by the U.S. Geological Survey. Many other methods have been derived to obtain the elements of the seismic moment tensor, for example, the one presented by Pearce and Rogers (1989) that uses the amplitude ratios of P, pP and sP. A different approach is followed by Vasco and Johnson (1990) who have devised a method of extreme models in the inversion of moment tensors to test how universal is the double-couple model and the presence of isotropic components.

A possible source of error in the determination of the seismic moment tensor is the misslocation of the hypocenter. Dziewonski et al. (1981) considered that the values given by hypocentral determinations from first arrival times may not be adequate for the determination of the seismic moment tensor. They proposed that the coordinates of the focus and the origin time must be determined at the same time that the elements of the moment tensor. This location of the focus does not correspond to the initiating point of rupture, but to the centroid of the source area. The method is called the inversion of the centroid moment tensor (CMT). The method uses the body wave portion of the seismogram and is solved in the time domain, computing the synthetic seismograms by superposition of normal modes and using a non-linear least-squares inversion. This method is actually used in a routine basis for large earthquakes using data from digital stations by the Harvard University group and reported in bulletins and periodic publications.

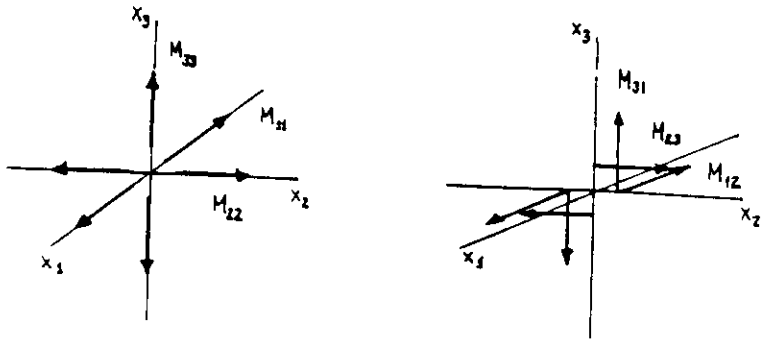

FIG. 2.1

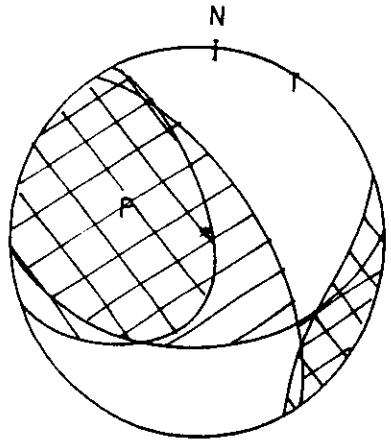

FIG. 2.2

3. SOURCE DIMENSIONS

3.1. Source time function

The first dimension that can be introduced in the representation of the source is that related to its dependence on time. As has been mentioned, the temporal dependence of the source can be represented by the source time function f(t). For a dislocation model, this function represent the time dependence of the non-elastic displacement or slip at the source $\Delta u(\xi,t)$. If the time dependence is the same at all points of the fault

$$\Delta u(t) = \Delta u\ f(t) \tag{3.1}$$

As was shown in (2.7) and (2.8), the displacements of the elastic waves at observation points away from the source depend on the derivative of the displacement at the source $\Delta\dot{u}(t)$, that is, the rate of slip or velocity of the displacement of each point of the source. This means that the radiation of energy from the source depends on the velocity and not on the displacement of the motion at the fault. Because of this reason, the term source time function is usually given to the derivative of f(t).

The simplest type of source time function if the Heaviside step function

$$f(t) = H(T) \begin{cases} = 0;\ t < 0 \\ = 1;\ t > 0 \end{cases} \tag{3.2}$$

This function does not introduce any time dimensions as the motion at the source occurs instantaneously from zero to its maximum value at time t = 0. The derivative of the H(t) function is the Dirac delta function $\delta(t)$. According to (1.8) and (1.9), the wave displacements u(t) will have in this case an impulsive form with this time dependence.

More realistic is to introduce a time τ, called the rise time, that takes for the displacement to reach from zero to its maximum value. This is the first way in which a dimension is assigned to the source. This time dimension may be considered even for point sources. The simplest function used in this case is a linear increase from 0 to τ,

$$\Delta u(t) = \begin{cases} \Delta u\ \dfrac{t}{\tau};\ & 0 < t < \tau \\ \Delta u\ ;\ & t > \tau \end{cases} \tag{3.3}$$

In this case, Δu increases linearly from zero to its maximum value in the time τ. The discontinous nature of this function can be avoided using an exponential dependency

$$\Delta u(t) = \Delta u\ H(t)\ (1 - e^{-t/\tau}) \tag{3.4}$$

In this case $\Delta u(\tau) = 0.63\Delta u$. In these two cases f(0) = 0. However, we are more interested in the behaviour of $\dot{f}(t)$, and in both cases for t = 0, this is not zero, but there is a jump in velocity. (Fig.3.1). One way to to avoid this problem is to use a function such that both f(t) and $\dot{f}(t)$ are zero at t = 0. This function can be approximated using for $\dot{f}(t)$ a triangular function. The form of the pulses of the seismic waves is the same as that of $\dot{f}(t)$ with a time width that depends on the rise time (Fig.3.2)

$$\Delta\dot{u}(t) = \begin{cases} 0\ ; & t < 0 \\ \Delta v\ t/\tau\ ; & 0 < t < \tau/2 \\ -\Delta v\ t/\tau\ ; & \tau/2 < t < \tau \\ 0\ ; & t > 0 \end{cases} \tag{3.5}$$

As we will see later, this function is generally used for modelization of wave forms. The form of the wave pulses are also triangular with a width depending on the rise time.If we want to introduce the duration of the process at the source keeping the point source approximation, we can make $\dot{f}(t)$ to have a trapezoidal shape with a total duration equal to T (Fig.3.3).

In conclusion, the time dimension in the source may be introduced by an appropiate choice of the source time function even if the source is kept to be punctual. This introduces new parameters such as the rise time and time duration. The wave

pulses resulting from this type of sources have a time width that depends on the time dimension of the source.

3.2 Source spatial dimensions

The point-source approximation does not consider the spatial dimensions of the source region. Progress in the representation of the seismic source must include besides its orientation, its shape and dimensions. One of the first relations between seismic waves and the dimensions of the source was established by Jeffreys (1931) who proposed a model of the source as a spherical cavity with uniform tensions applied on its surface. A similar model was also proposed by Nishimura (1937) and later by Scholte (1962) with a distribution of stresses over the surface of a sphere of finite radius.

Volume sources have little relation with the physical model of a fault. More realistic models start with the consideration of elastic dislocations of finite dimensions. Burridge and Knopoff (1964) studied the case of propagating dislocations over a certain finite length and showed its equivalence to propagating double couples. Previous to this work, Ben Menahem (1961, 1962) determined solutions for surface and body waves from extended sources, consisting in point forces of the single and double couple type propagating in one direction with a finite velocity v. The model of the fault is a rectangular fault of finite length L and width W. He shows that the effects of the finite dimensions can be isolated by means of the directivity function, ratio of the spectral amplitudes radiated from the source in opposite directions.

Haskell (1964, 1966) presented a model of the source with finite dimensions of rectangular shape of length L and width D, in which the slip has the form of a rupture front that propagates in one dimension with velocity v, along the length. The slip depends on time in such a way that takes a time τ (rise time) to reach its maximum value Δu in the form of a ramp function, from $t = 0$ to $t = \tau$ (3.3). This model has been used extensively to determine the dimensions of the source of earthquakes from the observations of seismic waves. Dimensions of the source were also introduced by Berckhemer (1962) for a circular fracture that propagates from its center, showing their influence in the width of the seismic pulse. Later, Berckhemer and Jacob (1968) calculated numerically the radiation for circular and rectangular faults initiating at a point and with variable velocity. A model of an elliptical fault was presented by Savage (1966). Rupture starts at one of the foci and propagate outwardly at constant velocity until the boundary is encountered with constant and variable slip. Hirasawa and Stauder (1965) investigated the radiation from several models of rectangular faults with fracture initiating at a point and propagating unilaterally and bilaterally.

The radiation of P waves in the far field, from a simple rectangular fault (Fig. 3.4), can be written in the form

$$u_l^P = \frac{\mu\, R(\gamma_l, n_l, l_l)}{4\pi\rho\alpha^3 r} \int_\Sigma \dot{\Delta u}\left(\xi,\ t - \frac{r}{\alpha}\right) dS \qquad (3.6)$$

Where $R(\gamma_l, n_l, l_l)$ is the radiation pattern of a point source as in expression (1.8), constant for Σ if r is very large in comparison with the dimensions of the source. If in the course of propagation, the fracture moves with velocity v along the length of the fault L, the integral can be written in the form

$$D \int_0^L \dot{\Delta u}\left[t - \frac{r}{\alpha} - \frac{\xi}{\alpha}\left(\cos\theta - \frac{\alpha}{v} \right) \right] d\xi \qquad (3.7)$$

For the time-dependence of Δu, the function (3.4) is used (Ben Menahem and Toksöz, 1963). In this case, taking the Fourier transform and evaluating the integral we obtained for the spectrum of the displacements

$$U_l^P(\omega) = \frac{\mu \Delta u\, LD}{4\pi\rho\alpha^3 r} R(\gamma_l, n_l, l_l) \frac{1}{1 + i\omega\tau} \frac{\sin X}{X} e^{i(\omega r/\alpha + X - \pi/2)} \qquad (3.8)$$

where X is given by

$$X = \frac{\omega L}{2\alpha}\left(\cos\theta - \frac{\alpha}{v} \right) \qquad (3.9)$$

In equation (3.8) the dimensions of the source introduce the factor $\sin X/X$ and the existence of a rise time the factor $(1 + i\omega\tau)^{-1}$. Therefore, the spectral amplitudes have the following form. For low frequencies as ω tends to zero the spectral amplitudes tend to a constant value. For values of ω larger than a certain value ω_c, the spectral amplitudes decrease as ω^{-2} (Fig. 3.5). The properties of the spectral amplitudes and phases for body and surface waves radiated from propagating sources over a finite fault area are the basis for the determination of the

parameters which define the dimensions of the source. These models introduce the following five parameters: L the fault length; D the fault width; v the rupture velocity; Δu the permanent slip and τ the rise time.

3.4 Corner frequency and dimensions

A different approach to the problem of fracture over an extended fault was presented by Brune (1970). He models the earthquake dislocation as a tangential stress pulse applied to the interior of a dislocation surface . The pulse is applied instantaneously over the whole fault surface, neglecting fault propagation effects. He described the near and far field displacement in the time and frequency domain. The spectrum has a flat part for low frequencies and decays as ω^{-2} for frequencies larger than a particular value ω_c called the "corner frequency" (fig. 3.5). This result agrees with the previous work by Aki (1967). The corner frequency is inverse proportional to the dimensions of the source. According to Brune , the radius of the circular fracture is related to the corner frequency of the spectrum of S waves by

$$r = \frac{2.21\ \beta}{\omega_c} \qquad (3.10)$$

Savage (1972) calculated the corner frequencies for P and S waves for a model of a rectangular fault of length L and width D and a rupture velocity $v = 0.9\ \beta$, with the following result

$$\sqrt{LD} = \frac{1.7\ \alpha}{\omega_c^P} \qquad (3.11)$$

$$\sqrt{LD} = \frac{3.8\ \beta}{\omega_c^S} \qquad (3.12)$$

According to these expressions, the corner frequency of the S waves is higher than that of the P waves. The opposite result is found from the model of Sato and Hirasawa (1973) and Molnar et al. (1973). According to Madariaga (1977), the form of the spectra with a decay as ω^{-2} beyond the corner frequency is a general property common to the large part of fracture models. However, the relation between the corner frequency and the fault dimensions depends on the details of the model assumed for the source, in

particular on the stopping mechanism.

3.5. Seismic moment and stress drop

As can be seen from equation (3.8), the displacements of seismic waves are proportional to the scalar seismic moment $M_0 = \mu \Delta u\ S$. This parameter can, then, be accurately determined from the observed seismic waves. It represents also a better measurement of the size of an earthquake than the magnitude and can be related to the stress drop at the source. The stress drop $\Delta\sigma$ is the difference between the shear stresses at the fault before and after the occurrence of an earthquake. For a circular fault of radius a, the relation between the seismic moment and the stress drop is

$$M_0 = \frac{16}{7} a^3\ \Delta\sigma \qquad (3.13)$$

In logarithm form the relation between the stress drop, the source area and the seismic moment for a circular fault is given by (Kanamori and Anderson, 1975)

$$\log M_0 = \frac{3}{2} \log S + \log \left(\frac{16\ \Delta\sigma}{7\ \pi^{3/2}} \right) \qquad (3.14)$$

For a constant $\Delta\sigma$, log S is proportional to log M_0 (Fig. 3.6). As an average, observations agree with this proportionality with slope 3/2 for moderate and large earthquakes. The stress drop may be considered constant with values ranging from 1 to 10 MPa (10 to 100 bars). This result was also found by Aki (1972). Larger values of stress drop seem to correspond to intraplate than to interplate earthquakes.

Seismic moment can be also related to magnitude, assuming an empirical relation between magnitude and energy. Using the Gutenberg-Richter relation for M_s , this relation is (Kanamori and Anderson (1975)

$$\text{Log } M_0 = \frac{3}{2} M_s - \log (\eta\bar{\sigma}/\mu) + 11.8 \qquad (3.15)$$

Where $\bar{\sigma}$ is the average stress acting at the source and η the seismic efficiency. Observations also support the constancy of the apparent average stress $\eta\bar{\sigma}$ with an average value of about 3 MPa (30 bars).

3.5 Nucleation, propagation and stop.

The complete process of fracture propagation from a kinematical point of view must include the description of its nucleation, spreading and stopping. Savage (1966) studied the effects on the seismic signal of the initiation and stopping of the rupture. The problem was more fully considered by Sato and Hirasawa (1973) and Molnar et al. (1973). In these models, the slip Δu was specified, in such a way, that it comes to a stop, when the limit of the fault is reached. The phase generated by the stopping of the rupture was called by Savage the "stopping phase". The relative importance of the initiating and stopping phases is different according to the model assumed for the slip.

In the simplest case, for a circular fault of radius a and displacement Δu constant over the entire fault surface, this may be represented by

$$\Delta u\ (\rho,t) = \Delta u\ H(t - \rho/v)\ [1 - H(\rho - a)] \qquad (3.16)$$

Where ρ is the radial coordinate and v the velocity of fracture propagation. In the center of the fault $\rho = 0$, the faults starts at time $t = 0$, in an instantaneous way from 0 to Δu. For a value $\rho < a$, Δu is zero until $t = \rho/v$, at this time arrives the fracture front that travels with velocity v. At the border of the fracture $\rho = a$, the motion stop ($\Delta u = 0$, for $\rho > a$) (Fig. 3.7). For a point at a distance r above the center of the fracture, an approximation of the displacements of P waves is

$$u(r,t) = 2\pi\ \Delta u\ v^2 (t - \frac{r}{v}); \quad v(t - \frac{r}{\alpha}) - a < 0$$

$$u(r,t) = 0; \qquad v(t - \frac{r}{\alpha}) - a > 0 \qquad (3.17)$$

The displacements have a discontinuity that corresponds to the time $t = a/v + r/\alpha$. According to our approximation this time corresponds to the arrival to the observation point to the signal from the stop of the fracture at the border ($\rho = a$). This arrival is called the stopping phase. After this phase the displacement is zero and there is an impulsive increase in velocity and acceleration.

The theory of propagating dislocations over a finite area has been also applied to the study of the near field displacements by Aki (1968), Haskell (1969) and other authors, using numerical integrations. A comparison of the near field motion for several different kinematic models of faulting can be found in Anderson and Richards (1975).

3.6 Modelling of seismic waves

Displacements of seismic waves as observed in a seismogram w(t) in a particular seismic station are the result of a convolution of the displacement at the focus u(t) with attenuation effects along the path Q(t) and the instrument response I(t)

$$w(t) = I(t) * Q(t) * u(t) \qquad (3.18)$$

Since I(t) is a known function and Q(t) for teleseismic distances ($\Delta > 30^\circ$) can be approximated by a linear operator F(t,T/Q) which satisfied that $T/Q = 1$ for P waves and $T/Q = 4$ for S waves, the time dependence of the seismic source can be obtained from u(t). In this way, the methods of seismic wave form modelling allow the determination of the source time function.

The method of modelling the forms of the waves consists in the calculation of theoretical seismograms from models of the source defined by its scalar seismic moment, orientation of the dislocation and the source time function. The comparison between the theoretical and observed seismograms permits to adjust the values of the parameters that define the seismic source.

Using a point source corresponding to a shear dislocation (DC), the vertical component of the P waves at a distance Δ, in spherical earth of radius a, may be written as

$$u_z^P = \frac{M_0}{4\pi\rho\alpha^3 a} R^P(\Phi, i_h) g(\Delta) c_z(i_0) f(t - r/\alpha) \qquad (3.19)$$

Where ρ is the density, α the P wave velocity, $R^P(\Phi, i_h)$ the radiation pattern for direct P waves which is a function of the relative orientation of the ray leaving the focus with respect to source geometry (i_h = take off angle at the focus) , $g(\Delta)$ the geometrical spreading of the wave front, $c_z(i_0)$ the free surface effect (i_0 = incidence angle at the station) and $f(t-r/\alpha)$ the source time function (Deschamps et al., 1980). Here the source time function $f(t)$ represent the time dependence of the slip velocity $\Delta\dot{u}(t)$.

If the focus is located at a depth h, besides the direct P ray we must considered the rays reflected in the free surface pP and sP that arrive at the station a short time later. (Fig. 3.9). Thus, we must modify expression (3.19),

$$u_z^P = \frac{M_0}{4\pi\rho_h \alpha^3 r_h} g(\Delta)\, c_z(i_0) \left\{ R^P(\Phi, i_h)\, f(t - t_p) + \right.$$

$$\left. + R^P(\Phi, \pi - i_h)\, v^{PP}\, f(t - t_{pp}) + R^{SV}(\Phi, \pi - j_h)\, v^{SP}\, f(t - t_{ps}) \right\}$$

(3.20)

The first term correspond to the direct P wave, the second to the pP and the third to the sP waves. In this expression R^P y R^{SV} are the normalized radiation patterns for the P and SV motion. For the pP and sP waves, the rays leave the source in upward direction and correspond to take-off angles equal to $\pi - i_h$. v^{PP} and v^{SP} are the reflection coefficients at the free surface for an incident P and S and reflected P. t_p is the arrival time of P, that is (r/α), t_{PP} y t_{SP} those of the pP y sP waves. These two last terms are given by

$$t_{PP} = t_P + \frac{2\, h \cos i_h}{\alpha_h} \qquad (3.21)$$

$$t_{SP} = t_P + h \left(\frac{\cos j_h}{\beta_h} + \frac{\cos i_h}{\alpha_h} \right) \qquad (3.22)$$

From these equations we can calculate the theoretical displacements of the P waves $u_z^P(t)$ for each station, that correspond to the sum of the three arrivals, namely, P, pP and sP (Fig.3.9). Depending on the depth of the focus h, the time intervals between these arrivals vary. For larger depths the intervals are longer and the aspect of the waves is more complex. The obtained displacements u(t) must be convolved with the response of the instrument I(t) and the attenuation factor of the medium Q(t), before we can compare the theoretical with the observed seismograms.

In practice, there are several computer programs to carry out the modelization (Deschamps et al., 1980; Helmberger, 1983; Nabelek, 1984). The technique that will be described corresponds to the method developed by Deschamps et al. (1980).

For each station, data used (limited to epicentral distances between 30° and 90°) are :The wave form of the vertical component of P (numerical sampled amplitudes given in cm), the take-off angle at the focus i_h, the azimuth Φ and the incidence angle at the station i_0, initial values of the orientation of the fault plane ϕ, δ y λ, depth of the focus h and of the source time function f(t) (usually of a triangular or a trapezoidal form). From these initial parameters starts the modelling process: First the theoretical seismogram is calculated for one station. This seismogram is compared with the observed. Using an iterative procedure the source parameters ϕ, δ, λ, h and f(t) are changed so that the best agreement possible is found between the theoretical and observed seismograms. The solution found for the first station is used for the other stations. By successive trials, a solution is found that adjust best to the greater number of stations. In this way, the depth of the focus h, and orientation of the fault plane, ϕ, δ, λ are corrected from the initial values (found from other methods such as arrival times and P wave polarities). Simple wave forms indicate surface shocks in very homogeneous media with a simple source, while complex wave forms may be due to deep focus, heterogeneous media or complex sources. An example of the ambiguity between the complexity of the source and the depth of the focus is shown in Figure 3.10. In this

figure the P waves in the same stations have been modelled using a simple source at a depth of 40 km and a complex source at a depth of 12 km. As can be seen, the effect is almost the same.

The problem of modelling wave forms at regional distances (epicentral distances between 50km and 1000 km) is more complex, since for this case the crustal and upper mantle structure has a great influence. The problem consists in separating correctly the effect of the source form the effect of the propagation in the medium. Correct detailed models of the crust and upper mantle are needed for each region that in most cases are not available (Helmberger y Engen, 1980; Koch, 1991; Sileny et al., 1992).

3.7. Empirical Green functions

To solve the problem proposed by the lack of knowledge about the detailed structure of the propagating medium, the method of the use of empirical Green functions has been proposed. This method is based on the use of waves from earthquakes of small magnitude as empirical Green functions, in order to model earthquakes of greater magnitude with the same hypocenter. It is assumed that the waves from the small earthquake include all the effects of the propagating medium and therefore are good approximations to the actual Green function, since its source may be considered approximately as a delta function (Mueller, 1985; Frankel y Kanamori, 1983; Frankel et al., 1986; Mori y Frankel, 1990).

Let us assume that $w_1(t)$ y $w_2(t)$ are the observed seismogram at the same station, for two earthquakes with the same hypocenter and different magnitudes. As we have seen, the seismogram is the result of a convolution of the displacement field generated at the source u(t), the propagating medium Q(t) and the instrument response I(t). The last two are the same for the two shocks.

$$w_1(t) = I(t) * Q(t) * u_1(t)$$
$$w_2(t) = I(t) * Q(t) * u_2(t) \qquad (3.23)$$

and in the frequency domain

$$w_1(\omega) = I(\omega)\ Q(\omega)\ u_1(\omega)$$
$$w_2(\omega) = I(\omega)\ Q(\omega)\ u_2(\omega) \qquad (3.24)$$

If the two earthquakes have the same mechanism, the radiation pattern is the same. The difference between the two signals is only due to the source time function. If the corner frequency of the smaller shock is greater than the range of frequencies in which we are interested, we can consider the waves of the smaller shock as generated by a Dirac delta function. The quotient of the seismograms in the frequency domain $w_1(\omega)$ and $w_2(\omega)$ in the frequency domain is the transform of the source time function of the larger shock.

$$\frac{w_1(\omega)}{w_2(\omega)} = \frac{u_1(\omega)}{u_2(\omega)} = F(\omega) \qquad (3.25)$$

If we take the inverse Fourier transform of F(w) we obtain the source time function f(t) of the earthquake of larger magnitude. From this function we can determine the seismic moment by calculating the area under the curve and the dimensions of the source from the time width or duration of the source function (Mori y Frankel, 1990).

Data needed for the application of this method are pair of seismograms in the same station from earthquakes with approximately the same hypocenter and mechanism and a difference in magnitude of at least one and maximum 2.5 units. The Fourier transform of the two signals must be calculated, then we make the quotient and take the inverse transform. The obtained signal which represent the source function is filtered. An example of this method is shown in Figure 3.11. The two earthquakes have magnitudes 3.2 and 4.5. The seismograms for each shock, their spectra and its quotient are shown. The source time function obtained has a duration of 0.56 s.

This method allows also to detect the directivity effects shown in differences of the signals observed at different stations for the same earthquake. Inspite of these differences the area under the signal which is a measure of the size of the shock must be the same in all stations.

This method is of great interest for the study of earthquakes

at regional distances, since it permits to separate the source and propagation effects. For this range of distances this is the only way to correct for the propagation in a very heterogeneous medium that never is known with sufficient detail. These shortcomings difficult the application at these distances the application of the modelling of wave forms.

3.8 Spectral analysis

As we have seen, the spectra of seismic waves depend on the dimensions of the source. For a great variety of models consisting on a fracture on a finite fault area, the shape of the spectrum has the same characteristics. These are: a flat or constant level of the amplitude spectrum for the low frequencies and a decay, generally, proportional to ω^{-2}, starting at the corner frequency ω_c (Fig. 3.5). The value of spectral amplitudes at the flat part is proportional to the seismic moment and the corner frequency to the inverse of the fault dimensions. It is possible, then, to determine these two parameters of the source from the seismic wave spectra.

The seismic moment can be obtain from body waves at teleseismic distances using the equation,

$$M_0 = \frac{\Omega_0 \, 4\pi\rho v_i^3 a \exp(\omega r / v_i Q_i)}{g(\Delta)\, c_i(i_0)\, R(\phi,\delta,\lambda,i_h)} \qquad (3.26)$$

Where Ω_0 is the spectral amplitude at the flat part of the spectrum of P or S waves, ρ the density at the focal region, v_i the velocity of P or S waves also at the focal region, a the radius of the earth, $g(\Delta)$ the geometrical spreading, the exponential function represents the attenuation of the medium (Q = quality factor), $c_i(i_0)$ the effect of the free surface and $R(\phi,\delta,\lambda,i_h)$ the radiation pattern. For regional distances $a/g(\Delta)$ may be substituted for r the distance along the ray.

The radius of a circular fault (Brune's model) can be calculated from the corner frequency f_c

$$r = \frac{2.34\ \beta}{2\pi f_c} \qquad (3.27)$$

For a rectangular fault (Haskell's model) we obtain from the corner frequency the product of the length L by the width D of the fault

$$\sqrt{LD} = \frac{1.7\ \alpha}{2\pi f_c} = \frac{3.8\ \beta}{2\pi f_c} \qquad (3.28)$$

From the values of M_0 and the dimensions r o L and D, other parameters of the fault such as the stress drop $\Delta\sigma$ and the average displacement $\Delta\bar{u}$ can be determined,

$$\Delta\sigma = \frac{M_0}{S^{3/2}} \qquad (3.29)$$

$$\Delta\bar{u} = \frac{M_0}{\mu\, S} \qquad (3.30)$$

Where S is the fault area and μ the shear or rigidity modulus at the focal region

Data needed for these calculations are digital recordings of P or S waves and the response function of the instrument. The observed signal w(t) is transformed to the frequency domain $W(\omega)$ (a minimum of 256 samples is recommended) The recorded signal has to be corrected by the instrument using the instrument response or transfer function. Usually the digital seismographs record velocities of ground motion. If these are given by s(t) (observed seismogram), they can be written in time and frequency domain as

$$s(t) = T(t) * v(t) \qquad (3.31)$$

$$\hat{s}(\omega) = \hat{T}(\omega)\hat{v}(\omega) \qquad (3.32)$$

Where T(t) is the response or transfer function of the instrument for velocity ground motion v(t). The ground displacement g(t) can be obtained by integration,

$$g(t) = \int v(t)\, dt \tag{3.33}$$

$$\hat{g}(\omega) = \frac{\hat{v}(\omega)}{i\,\omega} \tag{3.34}$$

$$\hat{s}(\omega) = \hat{T}(\omega)\; i\;\omega\;\hat{g}(\omega) \tag{3.35}$$

Therefore, in the frequency domain the ground displacement is given by

$$\hat{g}(\omega) = \frac{\hat{s}(\omega)}{\hat{T}_i(\omega)} \tag{3.36}$$

Where $\hat{T}_i(\omega)$ is the instrument transfer or response function for displacements. Although the data are velocities to determine the spectral amplitudes for displacements, we must use this transfer function. Usually transfer functions are given as quotients of polynomial form, specifying the poles and zeros. For example for a Streckeisen broad band instrument

$$\hat{T}_i(f) = \frac{2\,\pi\,i\,G}{f^2 - 2ihff_0 - f_0^2} \tag{3.37}$$

$$\omega = 2\,\pi\,f$$

Where $f_0 = 0.00278$ Hz, $h = 0.707$, $G = 1.04 \times 10^7$ counts/cm s^{-1}.

Once the spectrum has been corrected by the instrument, we can calculate the values of Ω_0 and f_c. In Figure 3.12 the P wave recorded in a short period instrument of vertical component is shown, together with the amplitude spectrum corrected for the instrument response. In the spectrum the values of Ω_0 and f_c are also shown..

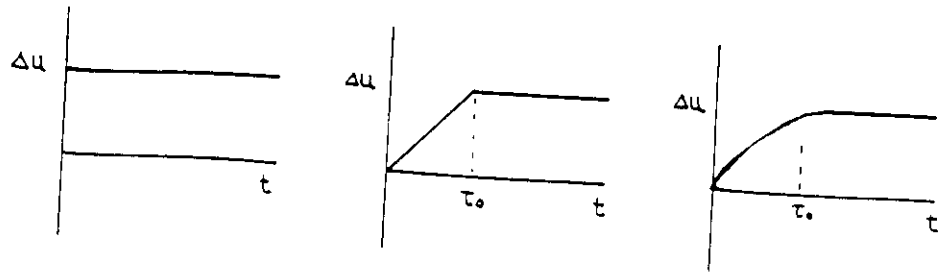

FIG. 3.1

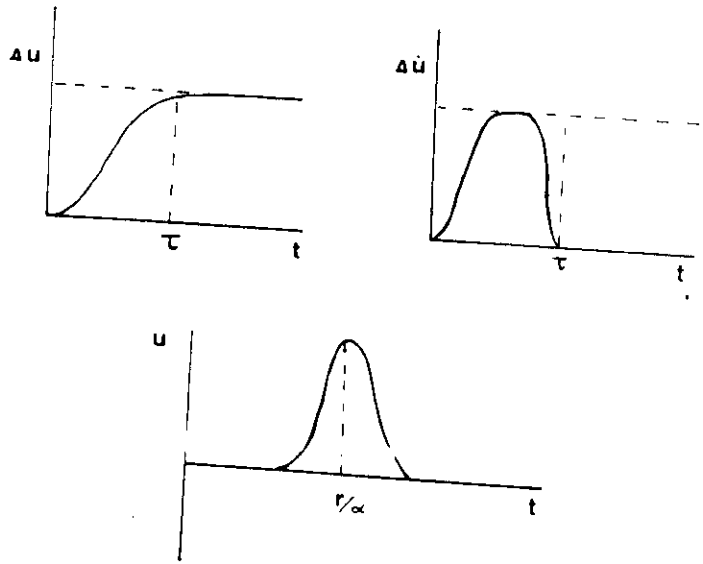

FIG. 3.2

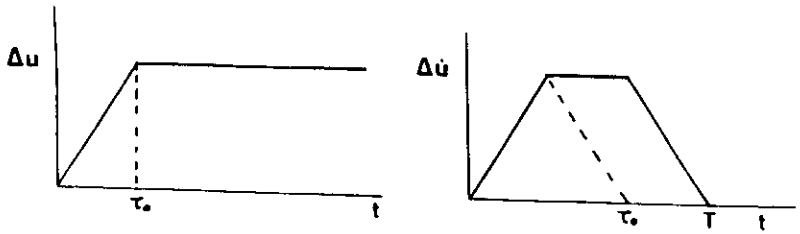

FIG. 3.3

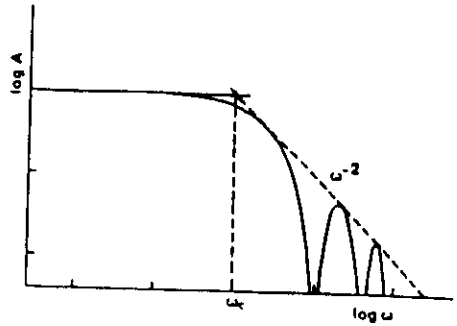

FIG. 3.5

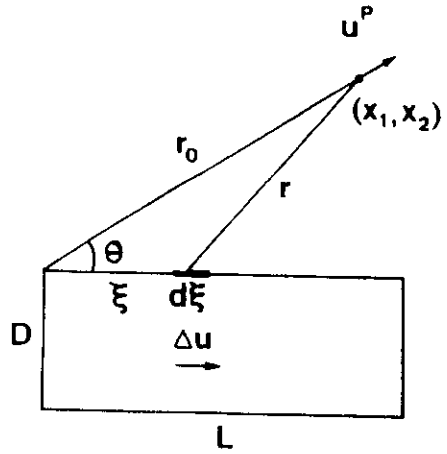

FIG. 3.4

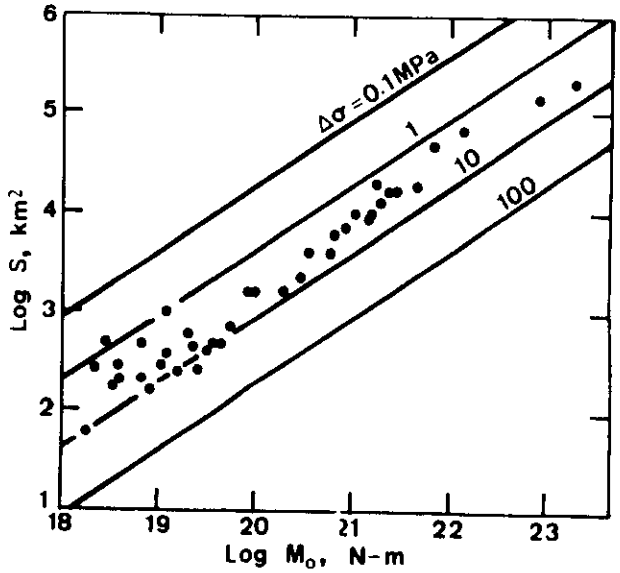

FIG. 3.6

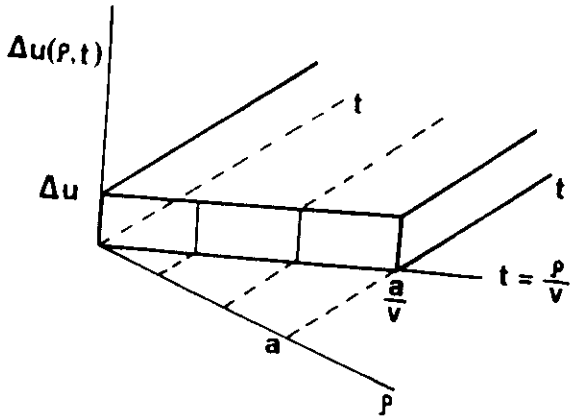

FIG. 3.7

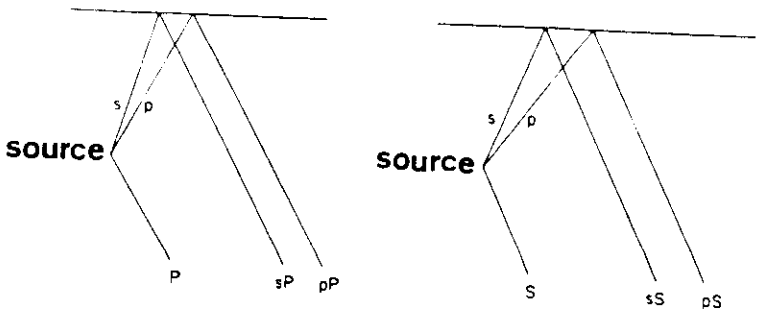

FIG. 3.8

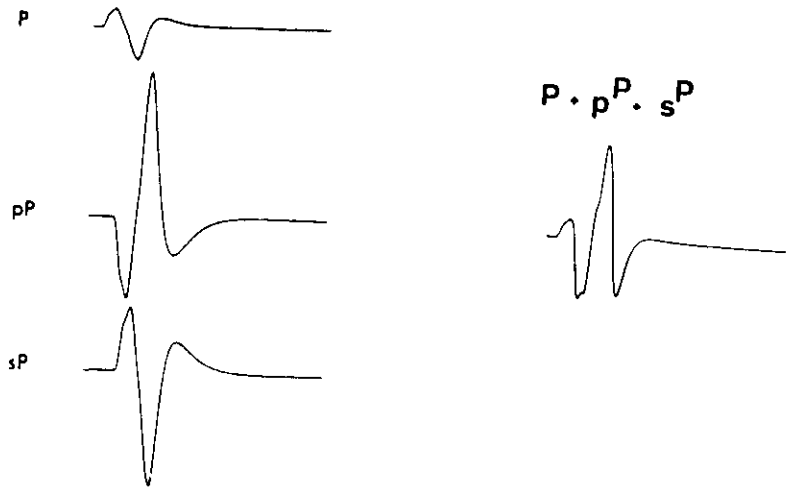

FIG. 3.9

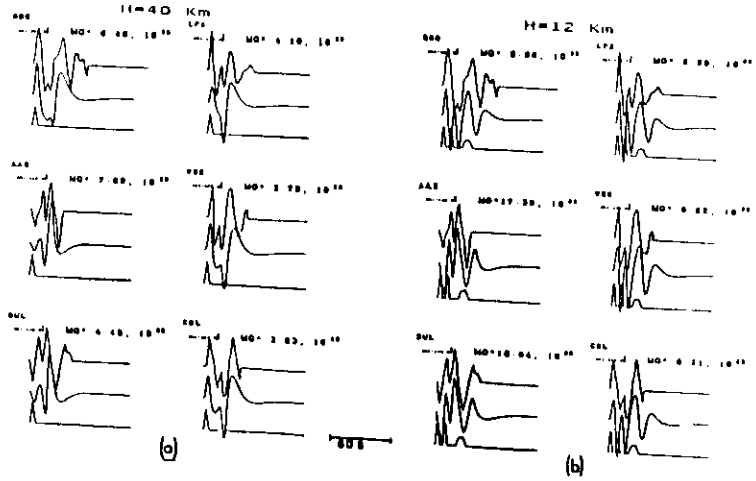

FIG. 3.10

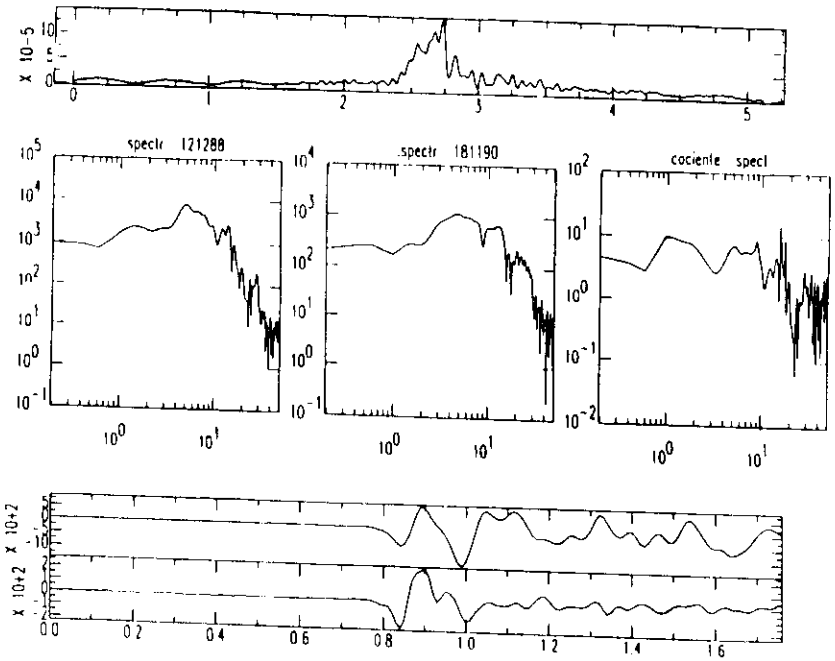

FIG. 3.11

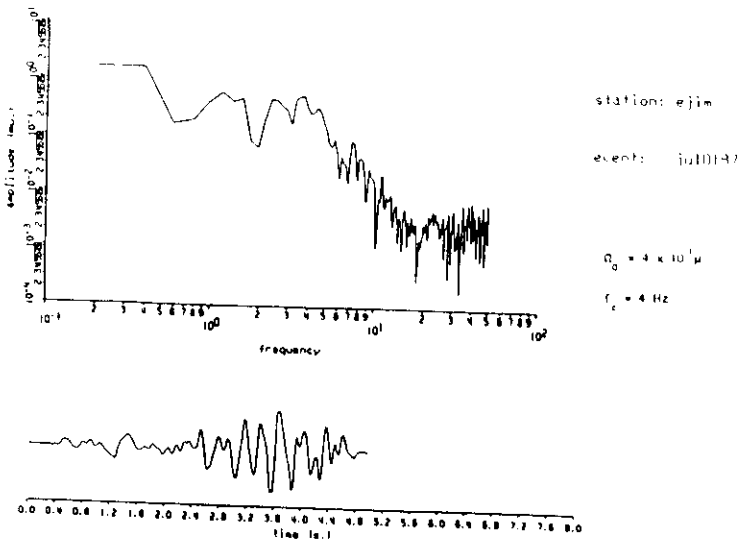

FIG. 3.12

4.DYNAMIC MODELS AND SOURCE COMPLEXITIES

4.1. Dynamic models

The kinematic models of the source mechanism of earthquakes are based on the assumption of a certain function of space and time for the slip $\Delta u(\xi_k,t)$ over the fault area. The form of the fault surface and the velocity with which Δu moves, that is, the velocity of fracture propagation must also be assumed in the model. The latter may be constant or variable over the fault. Depending on the model, the slip takes its maximum value at each point of the fault, either instantaneously or after a certain rise time as the fracture front propagates. The slip is also made to start at a certain point, propagate through the fault area and finally stop at its border. From these models, the displacement radiation $u(x_i,t)$ at the near and far field can be derived . From the physical point of view, the kinematic models have many shortcomings and inconsistencies. In fact, in them, near the borders of the fault there is interpenetration of matter, the strain energy drop is unbounded and the stress drop is infinite (Madariaga, 1976). To obtain more physically realistic models, one must proceed to establish dynamic models in which the slip is derived from the state of stresses and the strength of the material at the source region.

4.2. Stress drop and fault slip

The general problem of dynamic models is based on the idea of crack formation and propagation in a prestressed medium. The mechanism of an earthquake is considered as a shear rupture that nucleates at a certain point of the fault and propagates at a certain velocity and finally stops at its border. Inside the crack, the shear stress drops from its initial value σ_0 to a final value, defined as the frictional stress σ_F. The driving stress of the fracture is, then, the stress drop $\Delta\sigma$ or difference between the initial and residual values.

$$\Delta\sigma = \sigma_0 - \sigma_F \qquad (4.1)$$

The dynamic problem relates the displacement of the fault Δu with the stress drop $\Delta\sigma$. The simplest relation is that of the static solution, that for a total stress drop ($\sigma_F = 0$) in a circular fault gives

$$\Delta u(\rho) = \frac{\Delta\sigma}{\mu}\sqrt{a^2 - \rho^2} \qquad \rho < a \qquad (4.2)$$

The stresses outside the fracture due to the stress drop inside are

$$\sigma(\rho) = \frac{\Delta\sigma\ \rho}{\sqrt{\rho^2 - a^2}} \qquad \rho > a \qquad (4.3)$$

Expressions (4.2) and (4.3) introduced us in the dynamic problem. The slip Δu is not assumed as in the kinematic models, but results from the stress drop $\Delta\sigma$ over the fault area (Fig.3.1a). The stress drop on the fault modifies the state of stresses outside the fault, accumulating stresses near the border (Fig 3.1b). This creates a singularity where stresses become infinite.

The relation of $\Delta\sigma$ with the average value $\Delta\bar{u}$ is

$$\Delta\bar{u} = \frac{16a}{7\pi\mu}\Delta\sigma \qquad (4.4)$$

From this expression we can derive a relation between the scalar seismic moment and the stress drop

$$M_0 = \frac{16}{7}a^3\Delta\sigma \qquad (4.5)$$

For this case we can also write for the energy spent during the process in a fault of area S

$$E = \Delta\bar{u}\ \Delta\sigma\ S \qquad (4.6)$$

In terms of the seismic moment this expression can be written as

$$E = \frac{\Delta\sigma}{2\mu}M_0 \qquad (4.7)$$

If the stress drop is not total, there will be a residual energy lost by friction E_R, and the total energy, according to (4.5), will be

$$E = E_S + E_R = \Delta\bar{u}\ S\ (\Delta\sigma + \sigma_F) \qquad (4.8)$$

These simple relations show how we relate the displacement Δu at the fault with the stress drop $\Delta\sigma$, fraction of the stresses acting at the source region that is responsible for the displacement.

4.3 Crack or fracture propagation

The use of crack models for the dynamics of the source of earthquakes was initially proposed by Kostrov (1966). The physics of cracks can be traced back to the early work on the formation of cracks in crystals and metals by Griffith (1921), Starr (1928), Irwin (1948) and Orowan (1952). Kostrov (1966) laid the foundations of the dynamic problem for earthquake sources and found expressions for the slip inside the crack and stresses outside, both on the crack plane. Burridge (1969) extended Kostrov's work using a numerical technique to study finite shear cracks with a fixed velocity of rupture.

To study the propagation of shear cracks and their displacement fields for two dimensional models, two modes of shear fracture are considered antiplane and inplane (Fig. 4.2). In the antiplane mode, the slip along the surface of the crack is perpendicular to the direction of propagation of the rupture front. In this case, only SH motion is radiated. In the inplane mode, the slip is in the same direction as the rupture propagation and P and SV motion is generated. In the three-dimensional problem, both modes appear at different place around the fault boundary.

The simplest case of crack propagation is that of steady growth at constant rupture velocity in an homogeneous medium. In this case the crack propagates indefinitely. The growth of the crack is ensured by a finite energy flow into the rupture front. In this case the stress and slip velocity for the antiplane case, are given by (Madariaga, 1983)

$$\sigma(x) = K\ [x - l(t)]^{-1/2} \qquad (4.9)$$

$$\Delta u(x) = V\,[l(t) - x]^{-1/2} \qquad (4.10)$$

Where $l(t)$ is the position of the crack tip , K is the dynamic stress intensity factor and V the dynamic velocity intensity factor. The energy flow into the crack tip G, used to create new fault surface and which is spent in the processes in the breakdown zone, is given by

$$G = \frac{\pi}{2v} K V \qquad (4.11)$$

Where v is the velocity of rupture propagation. For antiplane cracks, K and V are related by the expression

$$K = \frac{\mu}{2v} (1 - v^2/\beta^2)^{1/2} V \qquad (4.12)$$

where μ is the rigidity and β , the shear wave velocity.

The natural fracture criterion demands that the energy flow into the crack tip be equal to the energy required to create a unit surface of new fracture.

The simplest models of crack propagation are those with an assigned velocity of rupture which may be given a constant value. In this case, if the crack starts at a point and growths symmetrically, without stopping, we have a circular crack. For this case, there is a simple relation for the shear slip Δu in terms of the shear stress drop $\Delta\sigma$ that drives the rupture process

$$\Delta u(r,t) = \frac{\Delta\sigma}{\mu} C(v) (v^2t^2 - r^2)^{1/2}, \qquad r < vt \qquad (4.13)$$

Where $C(v)$ is approximately unity for the whole subsonic rupture velocity range. The circular self-similar shear crack is very useful since it permits to study many properties of crack models.

If the slip, slip velocity and stress near the rupture front are examined (Fig. 4.3), it is found that the slip velocity inside the crack and the stress outside become infinite as they approach the rupture front. For brittle fracture where the material is either broken or continuous, with no transition zone , this is the situation (Kostrov and Das, 1988) . To avoid this singularity, a transition zone ahead of the crack tip must be considered. In this

zone there is an interaction of the material immediately ahead of the rupture front.

Barenblatt (1959) proposed a model with a transition zone that he called the cohesive zone, where cohesive forces act, opposing the crack sliding. This idea was applied to seismological models by Ida (1972) , Palmer and Rice (1973) and Andrews (1976) in the slip weakening model. This model assumes that the shear stress on the crack is a function of the slip. Several theoretical models have been proposed for the form of $\sigma(\Delta u)$. In all of them, the shear stress σ has a finite value for $\Delta u = 0$ and drops to the frictional stress for Δu larger than a critical value D (Fig. 4.4a). In general, as slip increases , the stress decreases from a certain value below which the crack does not slip to the frictional stress. In this model a breakdown zone of a certain length d is created which corresponds to the length of the cohesive zone along the crack front (Fig 4.4b). The size of this breakdown zone is thought to be very small compared to the overall dimensions of earthquake faults. A major difficulty with these models seems to be that the cohesive zone is not independent of the rupture history.

4.4. Spontaneous rupture, nucleation and stopping

Complete models of earthquake occurrence must include the entire phenomenon of rupture, its initiation or nucleation, propagation and stopping on the basis of the stress conditions and material properties at the source region. The two determining factor are , therefore, the tectonic stresses derived finally from the relative plate motions and the physical properties of the rocks at the fault zones.

To study the initiation and the spontaneous propagation of a fracture, a failure or fracture criterion must be introduced. For pure brittle fractures two criteria have been proposed (Kostrov and Das, 1988). Griffith's criterion states that in order to create new crack surface a certain amount of free surface energy is required that must be supplied from the surrounding medium . The specific amount of energy needed is assumed to be a material constant. Irwin's criterion is formulated in terms of the stress intensity factor. In order for the fracture to propagate the stress intensity factor must exceed a certain critical value. This criterion has been also formulated as a critical comparison of shear stress with a static friction level. If a cohesion zone is assumed to exist ahead of the crack tip, the failure criteria must be somewhat modified.

In models of spontaneous crack propagation, the stress distribution and the fracture criteria determine the motion of the crack tip. The first of these models was presented by Kostrov (1966) in analytical form for antiplane cracks in an infinite medium. This work was extended also to in-plane cracks by Burridge

(1969) applying numerical methods. Andrews (1976) used a finite differences technique to solve the problem, introducing the cohesive forces in the failure criterion. Madariaga (1976) used also finite differences to study the problem of a circular shear crack which growth at a fixed velocity and stops suddenly. Das and Aki (1977) used a numerical technique to determine the problem of two-dimensional shear crack propagation with a critical stress jump across the tip of the crack as the failure criterion.

The three-dimensional problem has been solved by several authors, such as Das (1981), Virieux and Madariaga (1982), and Day (1982) using numerical methods. For most models the average rupture velocity is controlled by the normalized strength and the complexity of the rupture process depends on the variations of stress and strength distribution.

If the conditions of stress and strength are homogeneous, once a fracture has been initiated, it will propagate indefinitely. In a model, however, a crack can be made to stop arbitrarily when the rupture front reaches a certain limit. For a circular crack, this can be made when the crack reaches a certain final radius (Madariaga, 1976). The stopping of rupture generates very strong healing waves that propagate inward from the edge of the fault that finally reduce the slip velocity to zero. A more realistic way to stop fracture propagation is to assume an inhomogeneous distribution of strength and stress (Husseini, et al., 1975). The crack tip motion can be stopped by a barrier of high surface energy along the fault plane or limiting the prestressed region to a finite size. The crack stops when the strength of the material to be fractured is too high or the stress drop on the crack is too low.

4.5. Complexity of the source

The study of wave forms generated by large earthquakes has shown that most of them are multiple events (Wyss and Brune, 1967). That is the source is not a simple fracture with uniform slip propagating at constant velocity over a certain area. The conditions over the fault surface cannot be homogeneous, even if only for the requirement of the rupture to stop at certain limits. Field observations show that faults cross over a variety of different kinds of rocks of different strength and that the fault surface changes directions at some places. If we want to describe the physical process of the rupture at earthquakes, the heterogeneity of the faulting process must, in some way, be modelled. Also, the fairly constant and relatively low values, between 1 and 10 MPa, obtained for the stress drops of earthquakes of magnitude above 5 , reveal that these must be average values over the whole fault, since rocks may support much higher stresses without fracturing. Observations in the near field at high frequencies show very complex seismic signals, also evidence of complex processes at the source.

Two models have been proposed to explain this heterogeneity and complexity of the source, the barrier and the asperity model. The barrier model proposed by Das and Aki (1977) and Aki (1979) assumes that faulting takes place under uniform prestressed conditions over the fault surface, but with differences in the strength. Regions of very high strength are called barriers since they will impede the propagation of rupture. Actually , when rupture arrives at a barrier it may stop temporarily and then continue if it is a weak barrier, or remain unbroken if it is a strong barrier. The stress will be released in the zones that have been ruptured and accumulate at the barriers left unbroken. After the earthquake, the fault area has a heterogeneous distribution of stress (Fig. 4.5). The faulting process consists, for this model, in several fractures separated by strong barriers. Large earthquakes are, then, a superposition of several smaller events. The barriers left unbroken may rupture later, giving origin to aftershocks after the occurrence of the main event.

In the model of asperities, proposed by Kanamori and Stewart (1978), the fault has a heterogeneous distribution of high and low prestressed zones. Zones or patches of high stress are called asperities. Previously to a large earthquake, the low strength zones of the fault rupture producing small events, leaving only the asperities, or zones of high strength where stresses are accumulated. These zones break during the main shock. Complexity of the source is produced by the successive rupture of several asperities. After the rupture of all the asperities, the stress falls to a uniform distribution over the fault (Fig. 4.5). This model explains the occurrence of foreshocks, but cannot explain the occurrence of aftershocks.

In the barrier model , an earthquake is a stress roughing process, while in the asperity model is a smoothing process. In both cases, however, earthquakes are complex ruptures of elementary patches, either of asperities or inter-barrier zones. A barrier model has been proposed by Papageorgius and Aki (1983) in which a rectangular fault is filled with circular cracks . In an earthquake, these cracks rupture progressively leaving the space between them (barriers) unbroken. In this model one can distinguish between the "global stress drop", estimated from the total fault area, assuming a uniform stress drop over the entire fault, and the "local stress drop", estimated from the maximum slip at each elementary crack. The presence of stable asperities and barriers through many repeated earthquakes may explain the concept of characteristic earthquakes (Aki, 1984). The complexity of the source may be also considered as the cause of departure from self-similarity in earthquakes. Self-similarity implies that the only parameter that regulates the earthquake process is the fault length. In complex sources the scale length of heterogeneities (barrier interval), the dimensions of the cohesive zone and the fault-zone width that are related to secondary features of the fault, such as branching, stepping, etc., are

important dominant factors (Aki, 1988).

Numerical models for complex sources have been applied by Mikumo and Miyatake (1978) for a fault with a variable distribution of friction and Day (1982) for fracture propagation in a medium with a nonuniform distribution of prestress. He considers the case of fracture in a fault with one or more asperities and the presence of friction. Das and Kostrov (1988) consider models with both asperities and barriers. They unify the terminology calling barriers, the localized regions of the fault which remain unbroken and asperities, those that rupture with a high stress drop. After considering many models, they conclude that the complexity of seismic radiation can be attributed to the inhomogeneity of stress drop distribution over the fault, the presence of barriers and of friction. It cannot be simply related to the number or size of the asperities. Complexity of the source may also be interpreted as caused by the non-planar geometry of the fracture. Andrews (1989) warns that planar thinking have dominated earthquake modeling and perhaps have led us astray. For him the essential mechanism in modeling earthquakes is geometric irregularity including fault-bends and fault-junctions.

4.6. Acceleration spectra

We have seen how the dimensions of the fracture affect the form of the amplitude spectra in the far field. Complexities of the fracture process, however, are only observed in the high frequencies observed in the near field. High frequencies attenuate very rapidly so that they are not observed in the far field. For the low frequency observations the source model of a uniform rupture over a certain fault area is adequate, but not so for the high frequencies. They are affected by the irregularities and complexities of the source, such as changes in the fracture propagation with stops and accelerations, existence of elementary units (asperities or barriers) that break progressively and departures from planarity in the fault surface.

Regarding the displacement spectrum (Fig. 3.5), the spectrum of accelerations is multiplied by a factor of ω^2. Its form, therefore, depends on ω^2 for the low frequencies, corresponding to the flat part of the displacement spectrum, and is flat for frequencies higher than the corner frequency ω_c. For higher frequencies a certain maximum frequency ω_{max} appear at approximately 10 Hz beyond which amplitudes decrease very rapidly (Fig. 4.6). This frequency is usually known as f_{max} ($\omega_{max} = 2\pi f_{max}$). This frequency has been related to attenuations effects in the path or to source effects. It is reasonable to think that both effects take part.

The source effects that have been related to f_{max} are in the

first place the minimum fracture dimension for elementary units of the fault (asperities or space between barriers). The source is conceived in these models as formed by a group of elementary units with a minimum dimension of about 200 m, that break successively. These units are easily associated to asperities. In this form f_{max} is a measure of the complexity of the fault. Aki (1988), associates f_{max} with the dimensions of the cohesive zone d or critical displacement D, in the form,

$$f_{max} \simeq \frac{v}{d} \simeq \frac{4\sigma_c v}{\mu\pi CD} \qquad (4.14)$$

Where v is the velocity of fracture propagation, σ_c the critical stress, μ the rigidity at the source and C(v) a function that for subsonic fracture has a value near to unity. The dimension of the cohesive zone may be between 100 m and 1 km. If v = 3 km/s and d = 300 m, f_{max} = 10 Hz.

Some authors (Madariaga, 1989) introduced another frequency called the "patch frequency" f_p, lower than f_{max} where there is a change in the slope of the spectrum. This frequency is related to the inverse of the dimension of the subevent fracture units. An earthquake is modelled by the rupture of one or several elementary fractures or asperities (patches). For small earthquakes, rupture of a single unit, the patch frequency coincides with the corner frequency, while for larger ones the patch frequency is higher than the corner frequency, but lower than the maximum frequency (Fig. 4.6). In this model the maximum frequency may not represent a source effect.

Source complexity and irregularity affects the radiation of high frequencies and for this reason can only be detected by the analysis of strong motion acceleration records from the near field. We have only shown the effects in amplitude spectra. Complex models of the source are used to model the strong motion records in a similar way as we showed the modelling of wave forms.

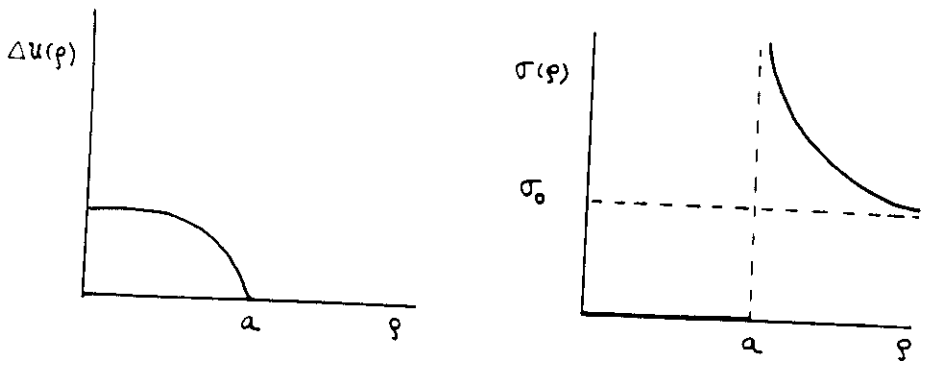

FIG. 4.1

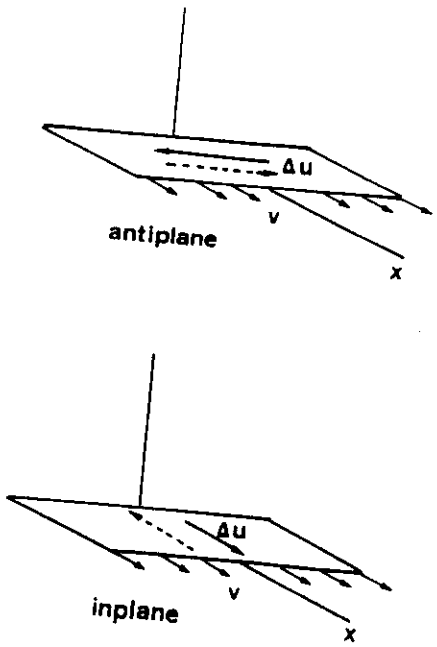

FIG. 4.2

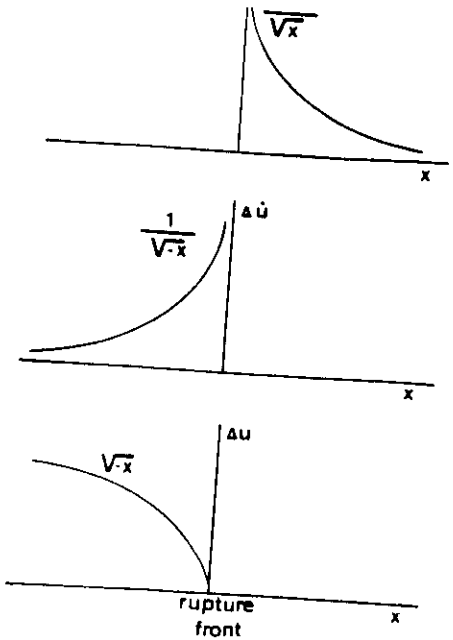

FIG. 4.3

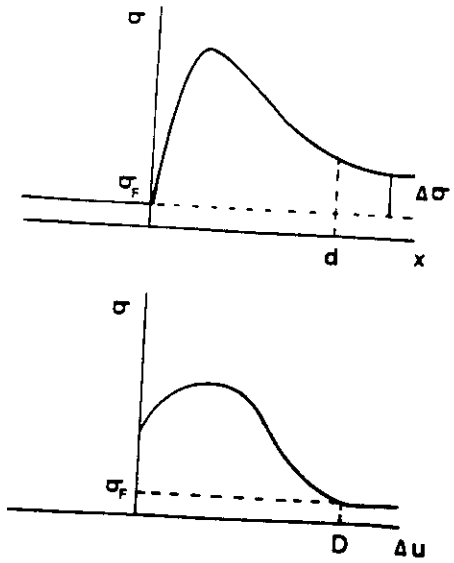

FIG. 4.4

REFERENCES

Aki, K., 1967. Scaling law of seismic spectrum. J. Geophys. Res. 72,1271-1231.

Aki, K., 1968. Seismic displacements near a fault. J. Geophys. Res. 73,5359-5376.

Aki, K., 1972. Earthquake mechanism. In: The Upper Mantle. A.R. Ritsema, ed., Elsevier, Amsterdam, 423-446.

Aki, K., 1979. Characterization of barriers on an earthquake fault. J. Geophys. Res. 84, 6140-6148.

Aki, K. 1981. A probability synthesis of precursory phenomena. In: Earthquake Prediction; An International Review. D.W. Simpson and P.G. Richards, eds., A.G.U., Washington, 566-574.

Aki, K., 1984. Asperities, barriers, characteristic earthquakes and strong motion prediction. J. Geophys. Res. 89, 5867-5872.

Aki, K. 1988. Physical theory of earthquakes. In: Seismic hazard in Mediterranean regions. J.Bonnin, M.Cara, A. Cisternas and R. Fantechi, eds., Kluwer Academic, Dordrecht, 3-33.

Aki, K. and P.G. Richards, 1980. Quantitative Seismology. Theory and Methods. W.H.Freeman, S. Francisco.

Anderson, J.G. and P.G. Richards, 1975. Comparison of strong ground motion from several dislocation models. Geophys. J. Roy. Astr. Soc. 42,347-373.

Andrews, D.J., 1976. Rupture propagation with finite stress antiplane strain. J. Geophys. Res. 81, 3575-3582.

Andrews, D.J., 1989. Mechanics of fault junctions. J. Geophys. Res. 94, 9389-9397.

Backus,G. and M. Mulcahy, 1976. Moment tensors and other phenomenological descriptions of seismic sources.I Continuous displacements. Geophys. J. Roy. Astr. Soc. 46,341-361.

Barenblatt, G.I., 1959. The formation of equilibrium cracks during brittle fracture. General ideas and hypothesis. J. Appl. Math. Mech. 23, 622-636.

Ben-Menahem, A. 1961. Radiation of seismic surface waves from finite moving sources, Bull. Seism. Soc. Am. 51, 401-453.

Ben-Menahem, A. 1962. Radiation of seismic body waves from finite moving sources in the earth. J. Geophys. Res. 67,396-474.

Ben-Menahem, A. and D.G. Harkrider, 1964. Radiation patterns of seismic surface waves from buried dipolar point sources in a flat stratified earth. J. Geophys. Res. 69, 2605-2620.

Berckhemer, H., 1962. Die Ausdehnung der Bruchfläche im Erdbebenherd und ihr Einfluss auf das seismiche Wellenspektrum. Gerland Beiträge zur Geophys. 71,5-26.

Berckhemer, H. and K. H. Jacob, 1968. Investigation of the dynamical process in earthquake foci by analysing the pulse shape of body waves. Inst. für Meteor. und Geophys. University of Frankfurt.

Brillinger, D.R., A. Udías and B.A. Bolt, 1980. A probability model for regional focal mechanism solutions. Bull. Seism. Soc. Am. 70, 149-170.

Brune, J.N., 1970. Tectonic stress and the spectra of seismic shear waves from earthquakes. J. Geophys. Res. 75, 4997-5009.

Buforn, E., 1985. Métodos para la determinación del mecanismo focal de los terremotos a partir de la polaridad de las ondas P. En: A. Udías, D. Muñoz y E. Buforn (eds). Mecanismo de los terremotos y tectónica. Universidad Complutense, Madrid, 117-139.

Buforn, E. and A. Udías, 1984. An algorithm for focal mechanism determination using signs of first motion of P, SV and SH waves. Rev. de Geofisica, 40, 11-26.

Burridge, R., 1969. The numerical solution of certain integral equations with non-integrable kernels arising in the theory of crack propagation and elastic wave diffraction. Phil. Trans. Roy. Soc. London A 265, 353-381.

Burridge, R. and L. Knopoff, 1964. Body force equivalents for seismic dislocations. Bull. Seism. Soc. Am. 54, 1875-1888.

Byerly, P., 1928. The nature of the first motion in the Chilean earthquake of November 11, 1922. Am. J. Sci. (series 5) 16, 232-236.

Das, S., 1981. Three dimensional rupture propagation and implications for the earthquake source mechanism. Geophys. J. Roy. Astr. Soc. 67, 375-393.

Das, S. and K. Aki, 1977. Fault planes with barriers: A versatile earthquake model. J. Geophys. Res. 82, 5648-5670.

Day, S.M., 1982. Three dimensional finite difference simulation of fault dynamics: Rectangular faults with fixed rupture velocity. Bull. Seism. Soc. Am. 72, 705-727.

de Hoop, A. T., 1958. Representation theorems for the displacement in an elastic solid and their application to elastodynamic diffraction theory. D.Sc. thesis, Technische Hogesschool, Delft.

Deschamps, A., H. Lyon-Caen and R. Madariaga, 1980. Mise au point sur les méthodes de calcul de sismogrammes synthétiques de longue période. Ann. Géophys. 36, 167-178.

Doornbos, D.J., 1982. Seismic moment tensors and kinematic source parameters. Geophys. J. Roy. Astr. Soc. 69, 235-251.

Dziewonski, A.M., T.A. Chou and J.H. Woodhouse, 1981. Determination of earthquake source parameters from waveform data for studies of global and regional seismicity. J. Geophys. Res. 86, 2825-2852.

Fitch, T.J., D.W. McCowan and M.W. Shields, 1980. Estimation of the seismic moment tensor from teleseismic body wave data with applications to intraplate and mantle earthquakes. J. Geophys. Res. 85, 3817-3828.

Frankel, A. and Kanamori, H., 1983. Determination of rupture duration and stress drop from earthquakes in southern California. Bull. Seism. Soc. Am. 73, 1527-1551.

Frankel, A.; Fletcher, J.; Vernon, F.; Haar, L.; Berger, J.; Hanks, T. and Brune, J., 1986. Rupture characteristics and tomography source imaging of $M_L \approx 3$ eartqhuakes near Anza, Southern California. J. Geophys. Res. 91, 12633-12650.

Geller, R., 1976. Body force equivalents for a stress drop source. Bull. Seism. Soc. Am.,66, 1801-1805.

Gilbert, F., 1970. Excitation of the normal modes of the earth by earthquake sources. Geophys. J. Roy. Astr. Soc. 22, 223-226

Gilbert, F., 1973. Derivation of source parameters from low-frequency spectra. Phil. Trans. Roy. Soc. A 274, 369-371.

Gilbert, F. and A.M. Dziewonski, 1975. An appliaction of normal mode theory to the retreival of structural parameters and source mechanisms from seismic spectra. Phil. Trans. Roy. Soc. A 278, 187-269.

Griffith, A.A., 1921. The phenomenon of rupture and flow in solids. Phil. Trans. Roy. Soc. London, A, 221, 163-198.

Haskell, N.A., 1964. Total energy and energy spectral density of elastic wave radiation from propagating faults. Bull. Seism. Soc. Am. 54,1811-1841.

Haskell, N.A., 1966. Total energy and energy spectral density of

elastic wave radiation from propagating faults. Part II. Bull. Seism. Soc. Am. 56,125-140.

Haskell, N.A., 1969. Elastic displacements in the near field of a propagating fault. Bull. Seism. Soc. Am. 59, 865-908.

Harkrider, D.G., 1964. Surface waves in multilayered elastic media, I. Rayleigh and Love waves from buried sources in a multilayered elastic half-space. Bull. Seism. Soc. Am. 54, 627-679.

Helmberger, D. V., 1983. Theory and application of synthetic seismograms. In: Earthquakes, Theory and Interpretation, H. Kanamori y E. Boschi (eds). North-Holland, Amsterdam, 174-222.

Helmberger, D. V. and Engen, G. R., 1980. Modelling the long-period body waves from shallow earthquakes at regional ranges. Bull. Seism. Soc. Am., 70, 1699-1714.

Helmberger, D.V., 1974. Generalized ray theory for shear dislocations. Bull. Seism. Soc. Am. 64, 45-64.

Hirasawa, T. and W. Stauder, 1965. On the seismic body-waves from a finite moving source. Bull. Seism. Soc. Am. 55,237-269.

Honda, H., 1962. Earthquake mechanism and seismic waves. J. Phys. Earth 10, 1-98.

Husseini, M.I., D.B. Jovanovich, M.J. Randall, and L.B. Freund, 1975. The fracture energy of earthquakes. Geophys. J. Roy. Astr. Soc. 43, 367-385.

Ida, Y., 1972. Cohesive force across the tip of a longitudinal shear crack and Griffith's specific surface energy. J. Geophys. Res. 77, 3796-3805.

Irwin, G.R., 1948. Fracture dynamics. In: Fracturing of Metals, American Soc. for Metals, Cleveland, 147-166.

Jeffreys, H., 1931. On the cause of oscillatory movements in seismograms. Month. Not. Roy. Astr. Soc. Geophys. Suppl. 2, 407-416.

Kanamori, H. and D.L. Anderson, 1975. Theoretical basis of some empirical relations in seismology. Bull. Seism. Soc. Am. 65, 1073-1095.

Kanamori, H. and J.W. Given, 1981. Use of long period surface waves for rapid determination of earthquake source parameters. Phys. Earth Planet. Int. 27, 8-31.

Kanamori, H. and G.S. Stewart, 1978. Seismological aspects of the Guatemala earthquake. . J. Geophys. Res. 83, 3427-3434.

Kasahara, K., 1963. Computer program for a fault-plane solution. Bull. Seism. Soc. Am. 53, 1-13.

Kawasumi, H., 1937. An historical sketch of the development of knowledge concerning the initial motion of an earthquake. Publ. Bur. Central Seism. Int. Ser. A, Trav. Scient. 15, 1-76.

Keylis-Borok, V.I., 1956. Methods and results of the investigation of earthquake mechanism. Bureau Centr. Seism. Int., Ser. A, Trav. Scient. 19, 383-394.

Keylis-Borok, V.I.,E.N. Bessonova, O.D.Gotsadze, I.V. Kirillova, S.D.Kogan, T.I. Kikhtikova, L.N. Malinovskaya, G.I. Pavlova and A.A. Sorskii, 1957. Investigation of the mechanism of earthquakes. Trudy Geofiz. Int. Akad. Nauk. SSSR, 40 (in russian).

Keylis-Borok, V.I., V.F. Pisarenko, J.I. Pyatetskii-Shapiro and T.S. Zhelankina, 1972. Computer determination of earthquake mechanism. In : Computational Seismology, V.I. Keylis-Borok, ed. Plenum, New York, 32-45.

Khattri, K., 1973. Earthquake focal mechanism studies-A review. Earth Sci. Rev. 9, 19-63.

Knopoff, L., 1961. Analytical calculation of the fault-plane problem. Publ. Dominion Obs. 24, 309-315.

Knopoff, L. and F. Gilbert, 1960. First motions from seismic sources. Bull. Seism. Soc. Am. 50,117-134.

Koch, K. , 1991. Momen t tensor inversion of local data. I. Investigation of the method and its numerical stability with model calculations. Geophys. J. Int. 106, 305-319.

Koning, L.P.G., 1942. On the mechanism of deep-focus earthquakes. Gerland Beitr. Geophys. 58, 159-197.

Kostrov, B. V., 1966. Unsteady propagation of longitudinal shear cracks. J. Appl. Math. Mech. 30, 1241-1248

Kostrov B.V. and S. Das, 1988. Principles of earthquake source mechanics. Cambridge U. Press.

Lamb, H. , 1904. On the propagation of tremors over the surface of and elastic solid. Phil. Trans. Roy. Soc. London. Ser. A 203, 1-42.

Love, A.E.H. ,1920. A treatise on the mathematical theory of elasticity (3rd edition) Cambridge U. Press.

Madariaga, R., 1976. Dynamics of an expanding circular fault.

Bull. Seism. Soc. Am. 66, 639-666.

Madariaga, R., 1977. High frequency radiation from crack (stress drop) models of earthquake faulting. Geophys. J. R. Astr. Soc. 51, 625-651.

Madariaga. R., 1983. Earthquake source theory: a review. In: Earthquakes: Observations, Theory and Interpretation. S.I.F. corso LXXXV, 1-44.

Maruyama, T., 1963. On the force equivalents of dynamical elastic dislocations with reference to the earthquake mechanism. Bull. Earthq. Res. Inst. 41, 467-486.

Maruyama, T., 1966. On two-dimensional elastic dislocations in an infinite and semi-infinite medium. Bull. Earthq. Res. Inst. 44, 811-871.

Mendiguren, J.A., 1977. Inversion of surface wave data in source mechanism studies. J. Geophys. Res. 82, 889-894.

Mikumo, T. and T. Miyatake, 1978. Dynamical process on a three dimensional fault with nonuniform frictions and near field seismic waves. Geophys. J. R. Astr. Soc. 54, 417-438.

Molnar, P., B.E. Tucker and J.N. Brune, 1973. Corner frequencies of P and S waves and models of earthquake sources. Bull. Seism. Soc. Am. 63,2091-2104.

Mori, J. and Frankel, A., 1990. Source parameters for small events associated with the 1986 North Palm Springs, California, earthquake determined using empirical Green functions. Bull. Seism. Soc. Am. 80, 278-285

Müller, G., 1985. The reflectivity method: a tutorial. J. Geophys., 58, 153-174.

Nabarro, F.R.N., 1951. The synthesis of elastic dislocation fields. Phil. Mag. 42, 1224-1231.

Nabelek, J.L., 1984. Determination of earthquake source parameters from inversion of body waves. Ph.D. Thesis, Massachusset Institute of Technology, Cambridge.

Nakano, H., 1923. Notes on the nature of forces which give rise to the earthquake motions. Seism. Bull. Centr. Meteor. Obs. Japan 1, 92-120

Nishimura, G., 1937. On the elastic waves due to pressure variations on the inner surface of a spherical cavity in an elastic solid. Bull. Earthq. Res. Inst. 15, 614-635.

Orowan, E., 1952. Fundamentals of brittle behaviour in metals. In:

Fatigue and Fracture of Metals, W.M. Murray, ed., J. Wiley, New York, 139-162.

Palmer, A.C. and J.R. Rice, 1973. The growth of slip surfaces in the progressive failure of over-consolidated clays. Proc. R. Soc. London A, 332, 527-548.

Papageorgious, A.S., and K. Aki, 1983. A specific barrier model for the quantitative description of inhomogeneous faulting and the prediction of strong ground motion. I. Description of the model. Bull. Seism. Soc. Am. 73, 693-722.

Pearce, R.G. and R.M. Rogers, 1989. Determination of earthquake moment tensor from teleseismic relative amplitude observations. J. Geophys. Res. 94, 775-786.

Randall, M. and L. Knopoff, 1970. The mechanism at the focus of deep earthquakes. J. Geophys. Res. 75,4956-4976.

Ritsema, A.R., 1955. The fault-plane technique and the mechanism in the focus of the Hindu-Kush earthquakes. Indian J. Meteor. Geophys. 6, 41-50.

Romanowicz, B., 1982. Moment tensor inversion of long period Rayleigh waves. A new approach. J. Geophys. Res. 87, 5395-5407.

Saito,M., 1967. Excitation of free oscillations and surface waves by a point source in a vertically heterogeneous earth. J. Geophys. Res. 72,3689-3699.

Sato, T. and T. Hirasawa, 1973. Body wave spectra from propagating shear cracks. J. Phys. Earth. 21, 415-431.

Savage, J.C., 1966. Radiation from a realistic model of faulting. Bull. Seism. Soc. Am. 56, 577-592.

Savage, J.C., 1972. Relation of corner frequency to fault dimensions. J. Geophys. Res. 77, 3788-3795.

Scheidegger, A.E., 1957. The geometrical representation of fault-plane solutions of earthquakes. Bull. Seism. Soc. Am. 47, 89-110.

Scholte, J.G.J., 1962. The mechanism at the focus of an earthquake. Bull. Seism. Soc. Am. 52, 711-721.

Sezawa, K. and K. Kanai, 1932. Amplitudes of P and S waves at different focal distances . Bull. Earthquake Res. Inst. 10, 299-334

Sileny, J.; Panza, G.F. and Campus, P., 1992. Waveform inversion for point source moment tensor retrieval with variable hypocentral depth and structural model. Geophys. J. Int. 109, 259-274.

Sipkin, S.A., 1982. Estimation of earthquake source parameters by the inversion of waveform data: synthetic waveforms. Phys. Earth Planet. Interiors 30, 242-255.

Sipkin, S.A., 1986. Interpretation of non-double-couple earthquake source mechanisms derived from moment tensor inversion. J. Geophys. Res. 91, 531-547.

Starr, A.T., 1928. Slip on a crystal and rupture in a solid due to shear. Proc. Cambridge Phil. Soc. 24, 489-500.

Stauder, W., 1962. The focal mechanism of earthquakes. Advances in Geophysics 9. 1-76.

Steketee, J.A., 1958. Some geophysical applications of the theory of dislocations. Canadian J. Phys. 36, 1168-1198.

Strelitz, R.A., 1978. Moment tensor inversions and source models. Geophys.J. R. Astr. Soc. 52,359-364.

Strelitz, R.A., 1989. Choosing the best double couple from a moment tensor inversion. Geophys. J. Int. 99, 811-815.

Stump, B.W. and L.R. Johnson, 1977. The determination of source properties by the linear inversion of seismograms. Bull. Seism. Soc. Am. 67,1489-1502.

Udías, A., 1991. Source mechanism of earthquakes. Advances in Geophysics 33, 81-139.

Udías, A. and Buforn, E., 1988. Single and joint fault-plane solutions from first motion data. In: D. Doornbos. Seismological Algorithms. Academic Press, Londres, 443-453.

Vasco, D.W. and L.R. Johnson, 1989. Inversion of wave forms for extreme source models with an application to the isotropic moment tensor component. Geophys. J. Int. 97, 1-18.

Virieux, J. and R. Madariaga, 1982. Dynamic faulting studied by a finite difference method. Bull. Seism. Soc. Am. 72, 345-369.

Volterra, V., 1907. Sur l'équilibre des corps élastiques multiplement connexes. Ann. Ec. Norm. Super. Paris, Ser. 3, 24, 401-517.

Vvedenskaya, A.V., 1956. Determination of displacements fields for earthquakes by means of the dislocation theory. Izves. Akad. Nauk. SSSR Ser. Geophys. 3, 277-284 (in Russian).

Vvedenskaya, A.V., 1959. The displacement field associated with discontinuities in an elastic medium. Izves. Akad. Nauk. SSSR Ser. Geophys. 4, 516-526 (in Russian).

Wickens, A.J. and J.H. Hodgson, 1967. Computer re-evaluation of earthquake mechanism solutions (1922-1962). Publ. Dominion Obs. 33, 1-560.

Wyss, M. and J.N. Brune, 1967. The Alaska earthquake of March 28, 1964: A complex multiple rupture. Bull. Seism. Soc. Am. 57, 1017-1023.

Yanovskaya, T.B., 1958. On the determination of the dynamic parameters of the focus hypocenter of an earthquake from records of surface waves . Izv. Akad. Nauk. SSSR, Ser. Geofiz. 209-301 (in Russian).